

Review

An Overview Analysis of Current Research Status in Iron Oxides Reduction by Hydrogen

Zuzana Miškovičová *, Jaroslav Legemza, Peter Demeter , Branislav Buľko , Slavomír Hubatka ,
Martina Hrubovčáková , Peter Futáš  and Róbert Findorák

Faculty of Materials, Metallurgy and Recycling, Technical University of Košice, 042 00 Košice, Slovakia; jaroslav.legemza@tuke.sk (J.L.); peter.demeter@tuke.sk (P.D.); branislav.bulko@tuke.sk (B.B.); slavomir.hubatka@tuke.sk (S.H.); martina.hrubovcakova@tuke.sk (M.H.); peter.futas@tuke.sk (P.F.); robert.findorak@tuke.sk (R.F.)

* Correspondence: zuzana.miskovicova@tuke.sk; Tel.: +421-55-602-3152

Abstract: This paper focuses on the study of current knowledge regarding the use of hydrogen as a reducing agent in the metallurgical processes of iron and steel production. This focus is driven by the need to introduce environmentally suitable energy sources and reducing agents in this sector. This theoretical study primarily examines laboratory research on the reduction of Fe-based, metal-bearing materials. The article presents a critical analysis of the reduction in iron oxides using hydrogen, highlighting the advantages and disadvantages of this method. Most experimental facilities worldwide employ their unique original methodologies, with techniques based on Thermogravimetric analysis (TGA) devices, fluidized beds, and reduction retorts being the most common. The analysis indicates that the mineralogical composition of the Fe ores used plays a crucial role in hydrogen reduction. Temperatures during hydrogen reduction typically range from 500 to 900 °C. The reaction rate and degree of reduction increase with higher temperatures, with the transformation of wüstite to iron being the slowest step. Furthermore, the analysis demonstrates that reduction of iron ore with hydrogen occurs more intensively and quickly than with carbon monoxide (CO) or a hydrogen/carbon monoxide (H₂/CO) mixture in the temperature range of 500 °C to 900 °C. The study establishes that hydrogen is a superior reducing agent for iron oxides, offering rapid reduction kinetics and a higher degree of reduction compared to traditional carbon-based methods across a broad temperature range. These findings underscore hydrogen's potential to significantly reduce greenhouse gas emissions in the steel production industry, supporting a shift towards more sustainable manufacturing practices. However, the implementation of hydrogen as a primary reducing agent in industrial settings is constrained by current technological limitations and the need for substantial infrastructural developments to support large-scale hydrogen production and utilization.

Keywords: decarbonization of metallurgical industry; low-carbon metallurgy; emissions; hydrogen as reducing agent; iron oxide reduction; hydrogen metallurgy; laboratory research



Citation: Miškovičová, Z.; Legemza, J.; Demeter, P.; Buľko, B.; Hubatka, S.; Hrubovčáková, M.; Futáš, P.; Findorák, R. An Overview Analysis of Current Research Status in Iron Oxides Reduction by Hydrogen. *Metals* **2024**, *14*, 589. <https://doi.org/10.3390/met14050589>

Academic Editors: Henrik Saxen and Zhengjian Liu

Received: 18 March 2024

Revised: 5 May 2024

Accepted: 15 May 2024

Published: 17 May 2024



Copyright: © 2024 by the authors. Licensee MDPI, Basel, Switzerland. This article is an open access article distributed under the terms and conditions of the Creative Commons Attribution (CC BY) license (<https://creativecommons.org/licenses/by/4.0/>).

1. Introduction

The steel industry is considered a crucial basic industry and plays a key role in strengthening the national economy. Characterized by high energy intensity, large production volume, and significant reliance on coal as the main energy source, the steel industry's energy demand and CO₂ emissions account for approximately 8% and 7% of the global totals, respectively [1–3]. The European Union's energy policy aims to reduce dependence on fossil fuels by promoting the use of renewable energy sources and carbon-free reagents [4–7]. Among these, hydrogen is particularly important and can also be used in iron and steel metallurgy technologies [8,9]. As an emission-free substance, hydrogen does not pollute the environment when released into the air, and is found in compounds such as water, natural gas, a mixture of hydrocarbons, and methanol. Hydrogen is an energy-rich fuel capable

of storing up to 33 kWh/kg and is considered the most promising clean energy of the 21st century due to its high calorific value, good thermal conductivity, and rapid reaction speed, making it highly suitable for application in iron and steel production [10,11]. Unlike natural gas or oil, hydrogen must be produced through energy-intensive processes [12]. Its full utilization demands significant economic resources and new investments, currently under intensive global research. Hydrogen offers a viable solution to decarbonize industrial processes and sectors where CO₂ emission reduction is critically important.

To lower CO₂ emissions in metallurgy, particularly in steel production, the industry has embraced not only hydrogen-based technologies, but also others technologies and strategies. Electric Arc Furnaces (EAFs) leverage electricity, potentially sourced from renewable energy, to melt scrap steel or direct reduced iron, drastically reducing CO₂ emissions compared to traditional blast furnaces that use coking coal. Additionally, Carbon Capture, Utilization, and Storage (CCUS) technology captures CO₂ emissions at steel plants and either stores them underground or utilizes them in other industrial processes to prevent their release into the atmosphere. The steel industry also focuses on enhancing energy efficiency through advanced process control, waste heat recovery, and upgrading older equipment. Using biomass as a renewable carbon source for iron ore reduction in blast furnaces significantly cuts CO₂ emissions compared to conventional coal and coke. Smelting reduction technologies like COREX and FINEX, which smelt iron ore directly with coal and oxygen, eliminate the need for coking and sintering plants, and reduce CO₂ emissions when combined with CCUS. Initiatives such as HYBRIT aim to use hydrogen produced from renewable energy for iron ore reduction, followed by steelmaking in an electric arc furnace, to achieve near-zero emissions. The industry also promotes the reuse and recycling of steel and optimizes resource use to minimize waste and lifecycle CO₂ emissions. Supporting these technological and process improvements, government policies including carbon pricing and subsidies for low-carbon technologies are crucial in encouraging the steel industry to adopt these environmentally friendly practices. These comprehensive efforts are designed to significantly reduce the environmental impact of steel production by incorporating advanced technologies, optimizing energy sources, and implementing sustainable material handling practices [13,14].

Currently, 96% of hydrogen produced originates from fossil sources, while 4% is derived from the electrolysis of water [1,15]. For large-scale hydrogen production for the steelmaking process, existing technologies such as methane reforming, gas from coke ovens, and coal gas are utilized. Additionally, new promising hydrogen production technologies are being developed. These include water electrolysis powered by renewable energy, biomass gasification, and hydrogen production using nuclear energy.

Despite its potential, H₂ has not yet been used on an industrial scale in iron production processes. However, its use as a reducing agent in the reduction of iron-bearing materials has been proven feasible and verified at the laboratory level [12]. Laboratory research into the reduction of iron ore using hydrogen is essential for developing more sustainable, energy-efficient, and ecologically acceptable methods for iron and steel production. These activities contribute to the industry's efforts to reduce carbon emissions and transition to cleaner, more efficient resource utilization methods. This paper provides an overview of research activities conducted within the framework of reducing iron-bearing materials using hydrogen.

The overall structure of this paper is divided into several parts. The first part describes applications of hydrogen in metallurgical processes and associated projects. The subsequent part provides an overview of laboratory research, detailing the methods and experimental conditions employed. Following this, the focus shifts to the results of the laboratory research. This Section offers detailed outcomes from various studies on hydrogen reduction, covering aspects such as thermodynamics, kinetics, and the influence of different conditions. The final part analyzes these findings, discussing the implications and potential of hydrogen use in the industry.

2. Application of Hydrogen in Metallurgical Technologies

Currently, hydrogen applications in the steel industry can be divided into three categories:

- As a reducing agent for the reduction of iron oxides, primarily used in the blast furnace process and the gas-based direct reduction iron (DRI) process.
- As fuel for heating, such as in the processes of sintering, pelletizing, or heating steel ladles.
- As part of protective atmospheres and prevention of oxidation of the processed material. During heat treatments like annealing and sintering, hydrogen is used to prevent metals from coming into contact with oxygen and other reactive gases in the atmosphere. This helps avoid corrosion or oxidation of metals during processing. During the heat treatment of carbon steels, hydrogen is also employed for their decarburization. For this purpose, a protective atmosphere consisting of a mixture of hydrogen and nitrogen is used [15–18].

The application of hydrogen for the reduction process in blast furnaces involves injecting a hydrogen-enriched medium into these furnaces. Given the characteristics of production in blast furnaces and the irreplaceable role of coke as the backbone of these processes, it is not feasible to completely replace coke and coal with hydrogen. However, with ongoing advancements in hydrogen metallurgy technology, it is anticipated that the substitution ratio of hydrogen for carbon will increase, aiming to reduce CO₂ emissions. This strategy represents a future direction for the development of the blast furnace ironmaking process [6,15,19].

The application of hydrogen metallurgy in the DRI process is predominantly associated with the gas-based DRI process, which currently represents more than 90% of global annual DRI production. The gas-based DRI technology is relatively mature, with the three main DRI processes—Midrex, HYL, and Finmet/FIOR—contributing approximately 75–80% to the total DRI output. Specifically, Midrex accounts for 60% of production, HYL for 15%, and Finmet/FIOR for less than 5% [19]. These processes are continually being developed and improved, as evidenced by innovations such as Midrex NG, Midrex H₂, and HYL/ENERGIRON [20,21]. These technologies utilize reducing gases primarily composed of hydrogen (H₂) and carbon monoxide (CO), produced by reforming natural gas. The primary aim of these advancements is to increase the hydrogen content in the synthesis, reducing gas to approximately 60–70%, and ultimately to achieve the use of nearly pure hydrogen (99.9%) for reducing iron ores and pellets. This shift focuses particularly on the adoption of green hydrogen, aligning with the principles of green metallurgy [15,22].

To reduce carbon emissions and advance H-DR (Hydrogen Direct Reduction) production in the steel industry, numerous significant projects, developments, and innovations involving hydrogen energy production and its application have been initiated. Currently, most of these projects are in the laboratory research phase, with only a select few metallurgical plants conducting tests with hydrogen in pilot operations [1]. Table 1 provides a summary of some ongoing projects, detailing their specific focus on the application of hydrogen in metallurgical processes.

Table 1. H₂ projects in metallurgy in the world.

Project	Country	Specification
H ₂ FUTURE	Austria, Germany, Netherlands	Initiated by Voestalpine, VERBUND, and Siemens, this project aims to produce green hydrogen using renewable electricity. This is accomplished through the operation of a 6 MW PEM electrolyzer located at the Voestalpine Linz steelworks [1].

Table 1. Cont.

Project	Country	Specification
H ₂ Green Steel	Sweden	The goal of this initiative is to establish a facility capable of producing green hydrogen, intended to replace natural gas in pig iron manufacturing and to electrify the entire process. The only emissions from this operation will be water vapor. Production is scheduled to commence in 2024 [1].
Carbon2Chem	Germany	This project focuses on converting by-product gases from the steel industry into chemicals such as ammonia, methanol, and polymers, while also recycling CO ₂ emitted during steel production [23].
SALCOS	Germany	The project aims to produce green hydrogen by using wind energy to electrolyze water, generating hydrogen and oxygen for use in iron production [23].
GrInHy 2.0	Germany	The project focuses on producing green hydrogen via high-temperature water electrolysis, utilizing electricity solely from renewable sources. It also harnesses waste heat from the steel industry to generate water vapor [1].
HYBRIT	Sweden	HYBRIT technology aims to replace coking coal in iron and steel production with emission-free electrical energy and hydrogen, striving to develop the world's first fossil fuel-free steel production technology [24].
ULCOWIN, ULCOLYSIS	EU's ULCOS project, which involved many European steelmakers	The ULCOS projects aims to electrolyze iron ore with zero carbon emissions [1].
HELIOS	Netherlands, Finland, Austria, Belgium	The project aims to train 10 doctoral candidates in green steel production using hydrogen. It combines research, internships, and mentorship from leading companies, universities such as KU Leuven and TU Delft, and research centers like K1-MET [25].
H ₂ STEEL	Italy, Netherlands, Spain, France	The EU-funded H ₂ STEEL project aims to transform organic waste and biomethane into green hydrogen, carbon, and essential materials using a novel catalytic pyrolysis technique in a new reactor. This approach facilitates cost-effective production [26].
HyInHeat	Spain, Italy, Finland, Belgium, Norway, Sweden, Germany, Greece, Austria, Netherlands	The EU-funded HyInHeat project aims to utilize hydrogen for high-temperature heating in the aluminum and steel industries. It focuses on redesigning processes and employing simulations to enhance energy efficiency and minimize hydrogen consumption [27].
Hybrid hydrogen-based reduction of Fe ores	Germany	The project combines hydrogen direct reduction (H-DR) and hydrogen plasma reduction (HPR) techniques to efficiently reduce and transform Fe ore, aiming to enhance energy and hydrogen utilization [28].
Hydrogen plasma-based reduction of Fe ores	Germany	The project focuses on researching the utilization of hydrogen plasma (HPR) [29].
HARARE	Norway, Greece, Germany, Belgium, Sweden	The HARARE project is dedicated to using hydrogen to recover metals and minerals from metallurgical waste, demonstrating sustainable, carbon-free methods for metal production and material valorization [30].
DRI expansion Project	China	Baosteel Zhan-jiang iron and steel project focused on the production of H-DRI at a volume of 1 Mt/year [31].

Perhaps the most renowned project globally is the HYBRIT project (Figure 1), which has developed the H-DRI (direct reduced iron with hydrogen) production technology. Initial experiments are currently being conducted at a pilot plant specifically for large-scale direct reduction using pure hydrogen. A preliminary study on direct hydrogen reduction was completed in 2017, finding that the proposed technology route is technically feasible

and economically attractive, particularly considering future trends in CO₂ emissions and electricity costs for northern Sweden/Finland. In February 2018, a decision was made to construct a 1 t/h pilot plant at SSAB's site in Luleå, Sweden, with construction commencing in June 2018 [24,32].

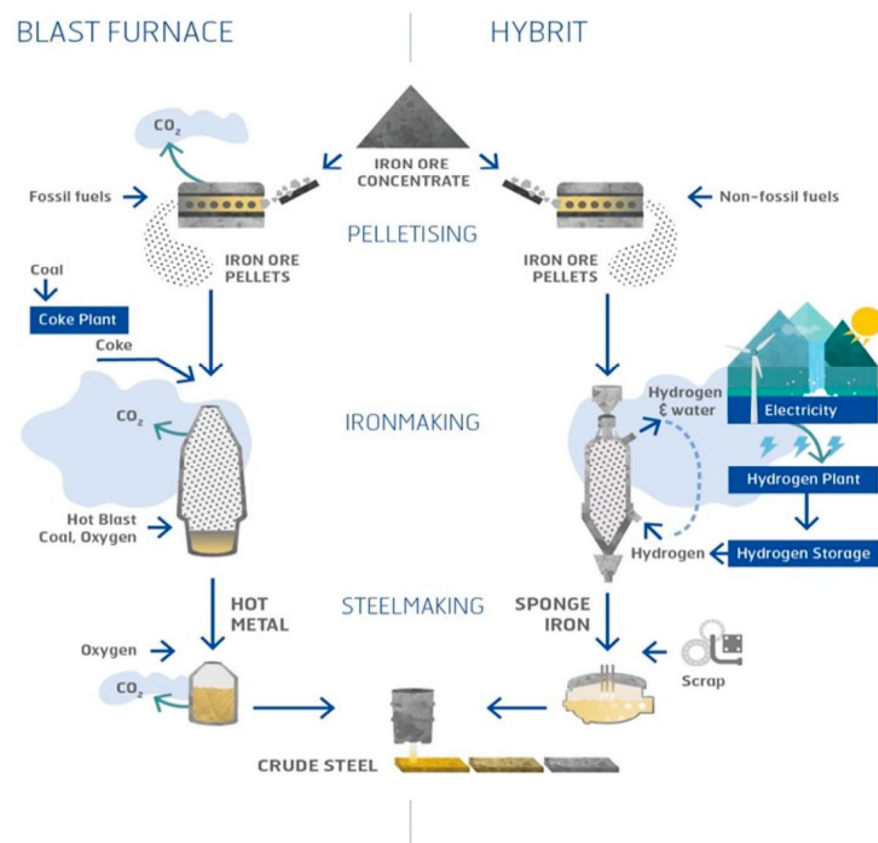


Figure 1. Blast furnace vs. HYBRIT technology Adapted from Ref. [24].

Currently, the project is in the phase of an experimental campaign for the production of H-DRI. The setup is designed to use hydrogen as the primary reducing gas, but remains flexible to accommodate other gases, such as biogas. Since 2016, a comprehensive four-year research program has been ongoing in Sweden, involving several research institutes and universities. This initiative aims to develop competence and knowledge across various domains, including the basic mechanisms of direct hydrogen reduction in iron ore (H-DRI), H-DRI smelting, innovative fossil fuel-free heating and agglomeration techniques, and hydrogen production and storage. It also focuses on balancing the electricity grid and supporting the steel industry's transition to carbon neutrality. In 2019, plans were initiated for the first demonstration plant for HYBRIT, scheduled to start operations in 2025 [24].

Engineering hydrogen-based iron reduction technologies, such as the HYBRIT initiative, involves overcoming several critical challenges. The process is notably energy-intensive, necessitating substantial renewable energy inputs to ensure sustainability. Developing a robust infrastructure for hydrogen production, storage, and transport is crucial, but also complex due to the stringent safety and efficiency requirements. Economic viability poses a significant concern, given the high costs associated with hydrogen production and the modifications needed for existing plants. Integrating new hydrogen processes into existing steelmaking operations requires meticulous engineering to maintain operational integrity and safety. Additionally, scaling up from pilot to full-scale production presents risks associated with technology scaling and system reliability. Moreover, managing hy-

drogen's high flammability necessitates strict safety protocols and adherence to regulatory standards [24].

2.1. Overview of Laboratory Research on the Reduction of Fe Materials by Hydrogen

Numerous studies globally have explored the use of hydrogen as a reducing agent. This article specifically focuses on laboratory research concerning the reduction of Fe-based metal-bearing materials, aiming to gather extensive information about the materials under investigation, furnace equipment, reduction conditions, and the influence of various parameters on the reduction process and the properties of the resulting products. Typically, laboratory experiments have concentrated on reducing ores, pellets, and synthetic powders. The sizes of the samples and their grain sizes largely depended on the capabilities of the experimental equipment available. Different methodologies were employed for the reduction in each type of material using hydrogen, reflecting the lack of a unified, standardized approach globally. Most experimental setups are characterized by unique, original methodologies developed by the researchers, tailored to the specific nature of the samples and the reduction parameters being monitored. Commonly used methodologies include those based on TGA (thermogravimetric) devices, fluidized beds, and reduction retorts, which rigorously monitor gaseous components, as shown in Figure 2 [33–35]. Another potential apparatus for reducing Fe materials with hydrogen is a rotary kiln. However, reports on the use of rotary kilns for the gaseous reduction of iron oxide are scarce, with this method occupying a niche between fixed bed and fluidized bed reactors [36].

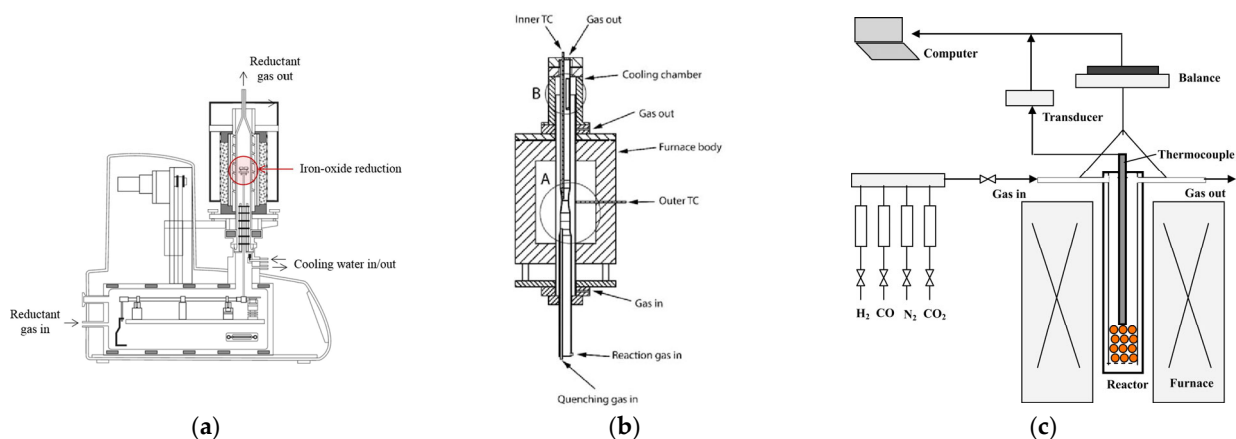


Figure 2. (a) TGA device. Reprinted with permission from ref. [33]. 2024 Elsevier; (b) fluidization device Adapted from Ref. [34]; (c) laboratory device with a retort. Reprinted with permission from ref. [35]. 2024 Elsevier.

Hydrogen flow rates in the experimental devices varied from 10 to 5000 mL/min, corresponding to the sample sizes ranging from 10 mg to 1000 g [37,38]. Typically, temperatures during hydrogen reduction were maintained within the range of 500–900 °C [39,40]. For specific experiments, depending on the studied material and the experimental objectives, hydrogen reduction was occasionally performed at higher temperatures, ranging from 1300 to 1600 °C [33,41]. Reaction times varied from 10 to 60 min, although some experiments extended up to 150 min [42–44].

The materials investigated in these studies (Table 2), which were reduced by hydrogen, can be categorized into:

- Fe ores/concentrates.
- Fe pellets.
- Fe synthetic powders.

Table 2. Generalized characteristics together with reduction conditions and equipment used for the investigated materials.

Researched Material	Fe Ores/Concentrates		Fe Pellets		Fe Synthetic Powders	
	Fluidization Device	Laboratory Device	TGA Device	Laboratory Device	TGA Device	Laboratory Device
Grain size	10–500 μm	44 μm –33 mm	8–15 mm	8–16 mm	1–5 μm	5 μm –5 mm
Sample weight	5–500 g	1–1000 g	-	-	10–20 mg	50 mg
Reaction time	4–60 min	30–150 min	120–150 min	45–120 min	-	-
Reaction temperatures	400–800 $^{\circ}\text{C}$	400–900 $^{\circ}\text{C}$	800–1100 $^{\circ}\text{C}$	700–1050 $^{\circ}\text{C}$	550–1580 $^{\circ}\text{C}$	25–900 $^{\circ}\text{C}$
Reducing gas	various ratios of H_2 : N_2 : CO ; pure gases H_2 , CO	various ratios of H_2 : N_2 : CO ; pure gas H_2	various ratios of H_2 : N_2 : CO ; pure gases H_2 , CO	various ratios of H_2 : CO : CO_2 : N_2 ; pure gas H_2	various ratios of H_2 : Ar : CO : H_2O ; pure gas H_2	various ratios of H_2 / N_2 , CO / N_2 ; pure gas H_2

In the studies, the ores were primarily reduced using self-constructed devices or within fluid reactors. For reduction processes in fluid reactors, a characteristic grain size below 500 μm is required to ensure stable fluidization of the ores. However, not all materials can be reduced using a fluidized bed due to their fluidization properties—the main limiting factor being the settling of particles [45]. The ores investigated typically consisted of hematite– Fe_2O_3 , with a total iron (Fe_{tot}) content ranging from 68% to 55% [46,47]. Iron pellets were reduced either in custom-built laboratory equipment or were closely monitored using TGA (Thermogravimetric Analysis) equipment. The iron pellets studied included both laboratory-prepared pellets and commercially produced industrial pellets [37,48,49].

The synthetic powders investigated in global studies were primarily in the form of nanopowders and included various compositions. These comprised Fe_2O_3 with a purity ranging from 99.5 to 99.9%, pure FeO , or mixed powders that combined several oxides and hydroxides [38,43,50].

The reducing atmospheres used in the experiments varied depending on the material being investigated and the specific objectives of the study. Most of the materials were tested either in an atmosphere of pure H_2 or in a mixture with the inert carrier gas N_2 [43,48]. A significant number of studies focused on comparing the reduction potential of pure reducing gases H_2 and CO [40,51]. Various mixtures of reducing gases were also examined, primarily H_2 : CO : N_2 mixtures, but experiments also included additional gaseous components such as CO_2 , $\text{H}_2\text{O}(\text{g})$, and CH_4 [35,52,53]. The impact of the concentration of individual gas components on the reduction parameters was carefully monitored. Table 3 is a compilation of selected publications that primarily lists the reduction parameters, devices, and materials investigated in individual laboratory researches.

Table 3. Publications focused on the reduction of Fe-based materials with hydrogen.

Fe Ores/Concentrates			
Material	Device/Reduction Parameters	Results	Reference
Iron ore–96.8% Fe_2O_3 sample weight: 8 g grain size: 106–150 μm	Fluidization device gas flow: 1.5 L/min reaction time: 4–60 min reaction temperatures: 600–800 $^{\circ}\text{C}$ reducing gas: H_2 , CO , N_2 in various mixtures	The reduction of fine-grained iron ore takes place more intensively with pure hydrogen than with pure CO or the H_2 - CO mixture.	Tao Zhang et al. [47]
Powder magnetite ore sample weight: 5 g	Fluidization device Inner diameter: 25 mm gas flow: 1000 mL/min reaction temperatures: 495–570 $^{\circ}\text{C}$ reducing gas: 80% H_2 : 20% N_2	The degree of reduction increased with the increase in reduction temperatures. The reaction rate increased as the reduction temperature increased.	Peiyu Li et al. [54]

Table 3. Cont.

Iron ore sample weight: 400 g grain size: 250–500 μm	Fluidization device Inner diameter: 68 mm gas flow: 25.9 NL/min reaction temperatures: 600–800 $^{\circ}\text{C}$ reducing gas: 65% H_2 : 35% N_2	Higher temperature increases the rate of reduction, especially in the intermediate and final stages of reduction.	Spreitzer D. et al. [45]
Fine-grained concentrate based on Fe_2O_3 sample weight: 170 g	Fluidization device Inner diameter: 26 mm Height: 160 mm gas flow rate: 0.2 m/s reaction temperatures: 500–600 $^{\circ}\text{C}$ reducing gas: H_2	The reduction yield for reduction in a fluidized bed using vibration ranged from 90 to 98% after approx. 50 min of reduction, while the increased frequency (47 Hz) supports the yield.	Shuo Li et al. [55]
Low-grade magnetite-based iron ore particle size ranges: 125–250 μm , 250–500 μm , and full size (mixed)	Fluidization device Inner diameter: 68 mm gas flow: 15.9 L/min reaction temperature: 700 $^{\circ}\text{C}$ reducing gas: H_2	Materials with higher temperature pre-oxidation treatment showed better fluidization behaviors. Lower pre-oxidation temperature is more beneficial for the reduction rate.	Zheng H. et al. [56]
Hematite ore grain size: 2 mm sample weight: 1 kg	Fixed bed reactor gas flow: 120 L/h reaction time: 30–150 min reaction temperatures: 400–500 $^{\circ}\text{C}$	At a reduction temperature of 500 $^{\circ}\text{C}$, the amount of reduced Fe_2O_3 increased rapidly at the beginning and then increased slowly. The reaction rate increased with increasing temperature.	Wenguang Du et al. [42]
Limonite Fe ore grain size: 44–89 μm sample weight: 5 g	Horizontal tube electric furnace Inner diameter: 16 mm Length: 950 mm gas flow: 200 mL/min reaction time: 30 min reaction temperatures 700–900 $^{\circ}\text{C}$ reducing gas: H_2 , N_2	SEM analyses of the partially and fully reduced particles showed that the iron oxide in the ore was reduced to metallic iron. As the reduction time increased, the reduced Fe formed a shell surrounding the unreacted oxides.	Zheng Wei et al. [36]
Hematite fine-grained ore grain size: 53–63 μm , 75–90 μm , 100–110 μm	Tube furnace Inner diameter: 100 mm Length: 1300 mm reaction time: 5–25 min reaction temperatures: 1450–1550 $^{\circ}\text{C}$ reducing gas: 40% H_2 : 60% N_2	The effect of particle size 53–110 μm on the degree of reduction is negligible.	Yingxia Qu et al. [46]
Low grade iron ore Grain size: 0.5–33 mm	Laboratory device gas flow: 0.5–1.5 L/min reaction time: 30–90 min reaction temperatures: 300–600 $^{\circ}\text{C}$ reducing gas: 100% H_2	Quantitative XRD analysis indicates that magnetite conversion is ~60% at 300 $^{\circ}\text{C}$, 100% at 400 $^{\circ}\text{C}$ with ~10% ferrite formation, and ferrite formation increased to ~90% at 600 $^{\circ}\text{C}$.	Nikhil Dhawan et al. [57]
Fe Pellets			
Material	Device/Reduction Parameters	Results	Reference
KRPS pellets CVRD pellets sample weight: 250 g	TGA device gas flow: 5 L/min. reaction time: 120 min reaction temperatures: 812/822 $^{\circ}\text{C}$ reducing gas: CO/H_2 in various ratios	Pellets reduced in H_2 swell easily due to the rapid phase transformation (hematite-magnetite-wüstite-iron) which is associated with the higher degree of reduction observed in H_2 .	Nyankson E. et al. [37]
Iron ore pellets from Outotec diameter: 10–13 mm sample weight: 3–3.7 g	TGA device gas flow: 1 L/min. reaction time: 150 min reaction temperatures: 800–1100 $^{\circ}\text{C}$ reducing gas: H_2 , CO	Higher reduction kinetics and thus higher raw material conversion are achieved in an H_2 atmosphere than in a CO atmosphere. In the presence of H_2 , the porosity is greater. The pellets are almost completely reduced to metallic Fe by H_2 at 800 $^{\circ}\text{C}$.	Scharm Ch. et al. [58]

Table 3. Cont.

Iron pellets with biomass and bentonite pellet size: 10 × 15 mm	Laboratory device gas flow: 7 cm ³ /s reaction time: 30 min reaction temperatures: 850–1050 °C reducing gas: H ₂ , N ₂	The time required to reach 99% reduction range is shorter when biomass is added to the pellets at the same reduction temperature, reflecting the accelerated rate of the reduction reaction.	Dabin Guo et al. [48]
Sintered pellets made of hematite powder–99.5% hematite	Laboratory device Inner diameter: 24 mm Height: 105 mm gas flow: 0.75 L/min reaction temperatures: 700–850 °C reducing gas: H ₂ /CO: 1.5	The reduction rate is higher for pellets with high porosity. Pellets with a lower density have a higher reduction range and reduction rate.	Dongchen Wang et al. [40]
Pellets diameter: 12 mm	Laboratory device gas flow: 5 L/min reaction temperatures: 800–1000 °C reducing gas: H ₂ /CO in various ratios	The rate of reduction was highest using H ₂ , the lowest rate was obtained using CO, and the rate of reduction using a gaseous mixture of H ₂ and CO was intermediate.	Hai-bin Zuo et al. [51]
Pellets from industrial production diameter: 10–12.5 mm sample weight: 500 g	Laboratory device gas flow: 15 L/min reaction temperatures: 700–1000 °C reducing gas: CO:H ₂ :N ₂ in various ratios	During the initial stages of reduction, the rate of reduction proceeds rapidly and the degree of reduction increases rapidly, then becomes less pronounced in the later stages due to the resistance of the product layer.	Qing Lyu et al. [59]
Fe pellets from Shouqin metal diameter: 10–12.5 mm sample weight: 500 g	Laboratory device Diameter: 75 mm Height: 800 mm gas flow: 12 L/min. reaction time: 45 min reaction temperatures: 760–1000 °C reducing gas: 75% H ₂ :25% N ₂	The highest degrees of reduction were recorded in the isothermal experiment at 900 °C.	Ming-Hua Bai et al. [35]
Fe Synthetic Powders			
Material	Device/Reduction Parameters	Reduction Parameters	Reference
Synthetically prepared samples of pure hematite	Electric resistance furnace gas flow: 70 cm ³ /min reaction time: 6–18 min reaction temperatures: 550–900 °C reducing gas: H ₂	The reduction in hematite to magnetite and the reduction in magnetite to wüstite are very fast. The slowest step in reduction reactions is the transformation of wüstite into iron.	Damien Wagner et al. [43]
Synthetic samples of α-Fe ₂ O ₃ , α-FeOOH, Fe ₅ HO _{8.4} H ₂ O, Fe ₃ O ₄ , FeO	TGA device gas flow–50 cm ³ /min reaction temperatures: 0–700 °C reducing gas: 5% H ₂ –95% Ar, 5% CO–95% Ar	Complete reduction in hematite to the metallic iron phase can be achieved even at a low temperature of up to 380 °C in pure hydrogen.	W.K. Jozwiak et al. [50]
Hematite powder sample weight: 0.013–0.019 g mean grain diameter: 0.74 μm	TGA device gas flow: 0.1 L/min reaction temperatures: 550–1300 °C reducing gas: H ₂ :CO in various ratios	The reduction rate in hematite particles increased with temperature, increasing H ₂ molecular fraction and atmospheric temperature. The reduction efficiency from Fe ₂ O ₃ to Fe was more than 99.9% above the temperature of 800 °C.	Jeongseog Oh et al. [33]
Laboratory prepared pure FeO sample weight: 20 mg	TGA device Inner diameter: 25 mm gas flow: 20 mL/min reaction temperatures: 900–1580 °C reducing gas: H ₂ gas flow: 20 mL/min	The reduction conversion tends to increase with increasing reduction temperature during the same reduction time, regardless of the phase state of the reactants and products.	Jianliang Zhang et al. [41]

Table 3. Cont.

Iron oxide Fe ₂ O ₃ : purity 97% sample weight: 50 mg	Analyzer Micromeritic Autochem 2920 gas flow: 20 mL/min reaction temperatures: 150–900 °C reducing gas: H ₂ :N ₂ , CO:N ₂ in various ratios	H ₂ is a better reducing agent than CO in the complete reduction of Fe ₂ O ₃ to Fe. CO is a more effective reducing agent to initiate the reduction.	Maratun Najiha Abu Tahari et al. [60]
Hematite powders: purity 99.5% sample weight: 50 mg	Laboratory device gas flow: 50 mL/min reaction temperatures: 25–600 °C reducing gas: 100% H ₂	During reduction at a heating rate of 20 °C/min, a phase transformation from a mixture of iron and magnetite to wüstite occurred already at a temperature above 510 °C.	Zhiyuan Chen et al. [38]
Iron oxide powder 40 wt% hematite (Fe ₂ O ₃), 58 wt% magnetite (Fe ₃ O ₄)	TGA device hydrogen partial pressure: 0.25–1 atm reaction temperatures: 400–900 °C reducing gas: H ₂ in various ratios	Full conversion to metallic iron was reached faster at 500 °C than at higher temperatures. Fewer, but larger pores were observed for reduction at higher temperature.	C.J.M. Hessels et al. [61]
Green compacts of hematite	TGA device gas flow: 1000 mL/min reaction temperatures: 500–1000 °C reducing gas: H ₂	The reduction of porous and dense samples reveals the presence of reduction rate minimum at 650 °C which was attributed to sintering and densification of the freshly reduced iron around the oxide grains.	El-Geassy et al. [62]
Hematite powder particle size: 74 µm	Tubular reduction furnace reaction temperatures: 600–1050 °C gas flow: 3.0 NL/min reducing gas: H ₂	The reduction rate of pure hematite with hydrogen linearly increased with temperatures from 600 to 1000 °C, without a rate minimum in this temperature range. Above 1000 °C, the reduction rate decreased due to sintering phenomena.	Junguo He et al. [63]
Single magnetite crystals	Tube furnace reaction temperatures: 900–1100 °C reaction time: 420 min reducing gas: H ₂	The reduction rate increases with reaction temperature. The reduction rate was found to be controlled by the solid-state diffusion mechanism.	Bahgat. M. et al. [64]

2.2. Results of Research Studies Focused on the Reduction of Iron Oxides with Hydrogen

2.2.1. Thermodynamics and Kinetics Basics of Reduction in Fe Oxides by Hydrogen

The reduction in iron oxides is a gradual process that significantly depends on temperature [65,66]. This thermodynamic behavior can be effectively visualized using a Baur–Glässner diagram, as depicted in Figure 3. The diagram illustrates the stable regions for different phases of iron oxides based on temperature and the degree of gas oxidation. The degree of gas oxidation is defined as the ratio of the oxidized components in the gas to the sum of oxidized and reducible gas components. From Figure 3, it is evident that the zone of stable iron expands with an increase in temperature when hydrogen is employed as the reducing agent. This observation suggests that higher temperatures enhance the efficiency of hydrogen in the reduction process. Conversely, the reduction behavior of iron oxides using the reducing gas CO exhibits an opposite trend, where lower temperatures may be more favorable [15].

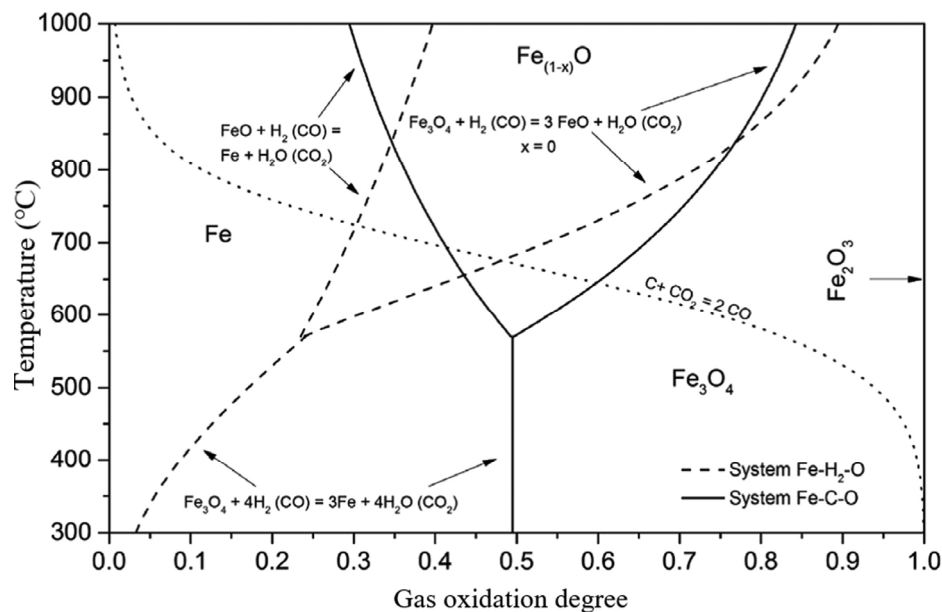
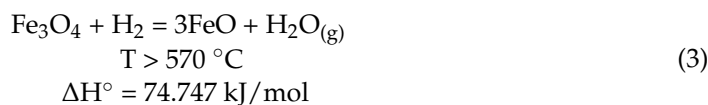
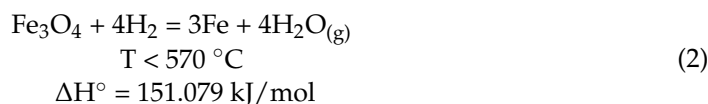
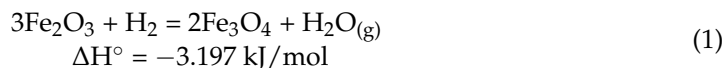


Figure 3. Baur–Glässner diagram for Fe-O-H₂ and Fe-O-C system including Boudouard reaction at 1 bar pressure and carbon activity 1. Reprinted with permission from ref. [15]. 2024 Elsevier.

The ratio of hydrogen to carbon monoxide in the reducing gas plays a crucial role in controlling the reduction rate. Thermodynamic calculations indicate that CO has greater reducing power at lower temperatures, whereas hydrogen reduction is more stable thermodynamically at higher temperatures. From a kinetic perspective, hydrogen atoms, due to their smaller size and higher diffusivity, act as a faster reducing agent than CO at temperatures above 850 °C. Thus, both thermodynamically and kinetically, increasing the temperature enhances the reduction of iron oxides with hydrogen [67].

Additionally, the reduction reaction of hydrogen is influenced by dynamic conditions. Factors that affect the reduction rate include temperature, pressure, gas composition, grain size, the porosity of iron oxide, and the mineralogy of the iron oxide [15,68,69]. These elements must be optimally managed to improve the efficiency and speed of the reduction process.

Kinetic studies have shown that the reduction in hematite progresses through sequential transformations, initially being reduced to magnetite, and then, at temperatures above 570 °C, it transitions to wüstite [66,70]. Below 570 °C, magnetite is directly reduced to iron as wüstite is unstable under these conditions. The first reduction reaction (hematite to magnetite) is slightly exothermic, allowing it to release some heat, whereas reactions (2) through (4) (magnetite to wüstite and wüstite to iron) are endothermic, requiring the input of heat to proceed [15].



As illustrated in Figure 4, the chemical reaction involves the adsorption of hydrogen gas at the iron oxide interface [71]. This interaction is a critical step in the reduction process, facilitating the transformation of iron oxide into iron.

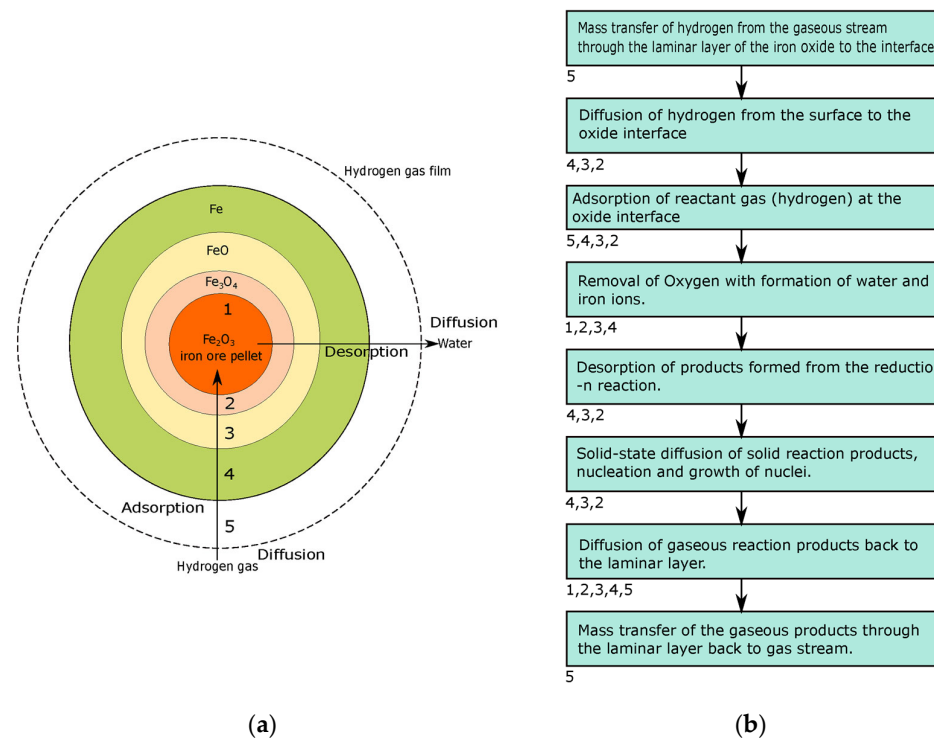


Figure 4. A reduction model showing the development of the reduction reaction of iron oxides with hydrogen; (b) Process steps in the reduction of iron oxides with hydrogen. The location of the process steps is shown by numbers 1 to 5 (b), which are also shown in the reduction model (a) Adapted from Ref. [71].

2.2.2. Influence of the Composition of the Reducing Atmosphere, Temperature and Kinetics on the Reduction in Fe Oxides by Hydrogen

The reduction potential of hydrogen (H₂) has been extensively analyzed across various studies, with the general consensus indicating that reduction with H₂ occurs more intensively and faster than with carbon monoxide (CO) or in an H₂/CO mixture [33,47,51,60,72–74]. Tao Zhang et al. observed a reduction in fine-grained iron ore using both H₂ and CO in their study. They noted that the reduction with H₂ was more intense, effectively reducing iron ore grains at both high (800 °C) and low temperatures [47]. Marathon Najih Abu Tahari et al. explored the effectiveness of H₂ and CO as reducing gases on iron oxides. Their findings highlighted that H₂ is a superior reducing agent compared to CO [60]. This observation was further supported by Jeongseog Oh et al., who monitored the rate of reduction of hematite particles in CO and H₂ atmospheres. They reported an increase in the reduction rate correlating with both higher temperatures and increased H₂ levels. At a temperature of 800 °C, the reduction efficiency of Fe₂O₃ to Fe exceeded 99.9% [33]. The studies also revealed that a higher reaction rate is achieved by increasing the H₂ content in the gas mixture, particularly at temperatures around 900 °C. This enhanced performance is attributed to hydrogen's superior reduction and diffusion capabilities compared to CO at temperatures above 890 °C [51].

The impact of hydrogen-based reduction gases (either pure or mixed gases) on the reduction process is crucial. This is primarily manifested in the reduction and diffusion capacity of the used reduction gases.

Zuo et al. found that when using pure H₂, the diffusivity and chemical reaction rate increase with temperature, and the increase in the reduction rate constant with rising tem-

perature is amplified with increasing hydrogen content. The effective diffusion coefficient is determined by the temperature and the physical properties of the gas. With increasing temperature and H_2 content, the diffusion coefficient also increases. Mixing just a small amount of CO into a H_2 reducing gas mixture drastically decreases the diffusion coefficient. However, the reaction rate constant is not as negatively affected as the diffusion coefficient when CO is introduced into a hydrogen gas mixture, according to Zuo et al. The reason for this could be that it only takes a small amount of CO molecules to reduce the fluidity of the gas and block the diffusion path, due to the higher viscosity and molecular size of CO, thus hindering H_2 from reducing the iron oxides, while the reaction rate constant remains largely unaffected [51].

Incorporating nitrogen (N_2) into a hydrogen (H_2)-reducing gas mixture for processing iron (Fe) materials impacts the process both practically and chemically. Nitrogen, being inert under standard iron reduction conditions, does not engage in chemical reactions. It serves as a diluent when combined with hydrogen, lowering hydrogen's partial pressure. This dilution effect diminishes the overall rate of hydrogen's reaction with iron oxides due to a reduced concentration of active hydrogen. Moreover, nitrogen's distinct thermal properties, such as specific heat capacity, modify the reactor's thermal dynamics. It influences how heat is absorbed, retained, and distributed within the gas mixture and the ore, potentially impacting temperature stability and, consequently, the kinetics of the reactions. In industrial applications, nitrogen helps regulate the flow and distribution of the reducing gases within the reactor. This regulation is crucial for maintaining consistent conditions throughout the ore bed, promoting uniform reduction throughout the batch. Economically, using nitrogen to dilute hydrogen in the gas mix reduces costs since nitrogen is generally cheaper than hydrogen. Additionally, nitrogen's use increases safety by lowering the risk of flammable conditions due to hydrogen's high flammability [35,75].

One of the most critical factors influencing the hydrogen reduction of iron oxides is the temperature at which the reduction occurs [76]. The process is significantly more intensive at higher temperatures, around $800\text{ }^\circ\text{C}$, which notably enhances both the reaction rate and the degree of reduction; increasing the temperature tends to increase these parameters. Conversely, certain Fe ore grains are effectively reduced even at lower temperatures, approximately $600\text{ }^\circ\text{C}$ [47,77]. This observation is supported by the findings of Damien Wagner et al., who conducted a study on the reduction of hematite powder at various temperatures. Their results showed that the highest rate of reduction occurred at the maximum temperature studied, which was $900\text{ }^\circ\text{C}$ (illustrated in Figure 5) [43].

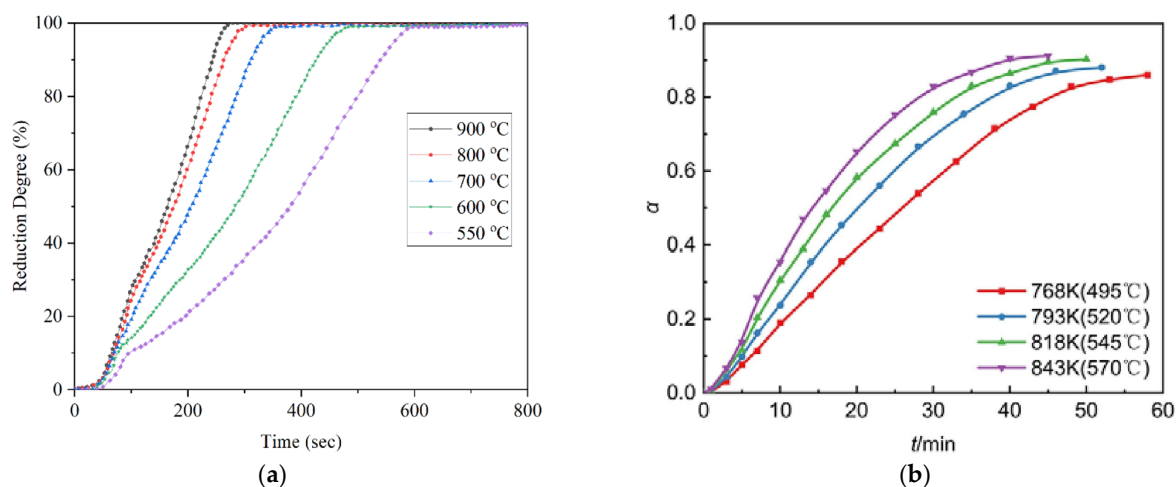


Figure 5. Effect of temperature on the rate of reduction: (a) of hematite powder at temperatures above $550\text{ }^\circ\text{C}$ Adapted from Ref. [67]; (b) of magnetite ore at temperatures below $570\text{ }^\circ\text{C}$. Reprinted with permission from ref. [54]. 2024 Elsevier.

The degree of reduction (degree of conversion) increases with the reduction temperature during the same duration, irrespective of the phase state of the reactants and products [41,78]. However, a critical temperature to consider is 570 °C, which marks the lowest limit for the thermodynamic stability of FeO. Under specific hydrogen reduction conditions, complete reduction of hematite to metallic iron can occur even at temperatures as low as 380 °C in pure hydrogen [50]. When reducing magnetite to metallic iron below 570 °C, the resulting product is porous, which beneficially impacts the reduction by decreasing the gas diffusion resistance [54]. Kun He et al. observed the reduction in hematite concentrate from Brazil in a fluidized bed at temperatures up to 570 °C. Notably, the FeO phase was absent in the final product, indicating that the reduction proceeded through the $\text{Fe}_2\text{O}_3\text{-Fe}_3\text{O}_4\text{-Fe}$ pathway [79].

While temperature plays a crucial role in the formation of FeO during reduction, the conditions under which heat is conducted (e.g., heating rate) are also vital. Zhiyuan Chen et al. explored the effect of heating rate on hematite powder (99.5% purity). They found that at a heating rate of 20 °C/min, the FeO phase appeared at 510 °C. Conversely, at a slower rate of 10 °C/min, the FeO phase was not detected (illustrated in Figure 6) [38].

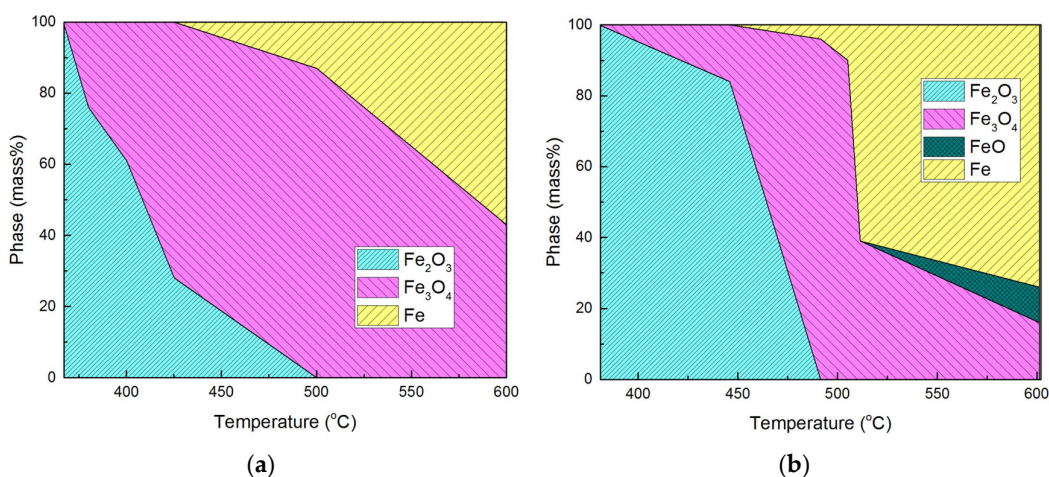


Figure 6. Calculated mass ratio of phases from XRD data according to the Chung model in samples partially reduced with pure hydrogen at heating rate: (a) 10 °C/min; (b) 20 °C/min Adapted from Ref. [38].

Generally, the reduction from Fe_2O_3 to Fe_3O_4 and from Fe_3O_4 to FeO occurs rapidly. The transformation of FeO to metallic Fe is the slowest step in the reduction reactions [43]. Initially, the reduction rate is high, and the degree of reduction quickly increases, but the rate becomes less pronounced in the later stages due to the resistance offered by the product layer [59]. Oscar Hessling et al. investigated the kinetics of reducing fine-grained materials based on hematite and discovered that the reduction rapidly reaches an O/Fe ratio of 0.5 within 120 s at 615 °C, but subsequent reduction slows due to the sluggish diffusion processes. SEM micrographs of reduced and partially reduced samples indicate that gas diffusion controls the reaction at later stages [34]. This finding is corroborated by Emmanuel Nyankson et al., who studied the kinetics of ferrous pellet reduction. They reported that the initial phase of reduction is governed by an interfacial chemical reaction, while the later stages are dominated by diffusion [37]. During the reduction of FeO to metallic Fe, the resulting metallic iron forms a dense structure that impedes diffusion and mass transfer, making it challenging for oxygen to pass through the dense iron layer (as depicted in Figure 7). Conversely, the reduction in Fe_3O_4 to metallic Fe below 570 °C produces a more porous product, which positively affects the reduction by lowering gas diffusion resistance [54].

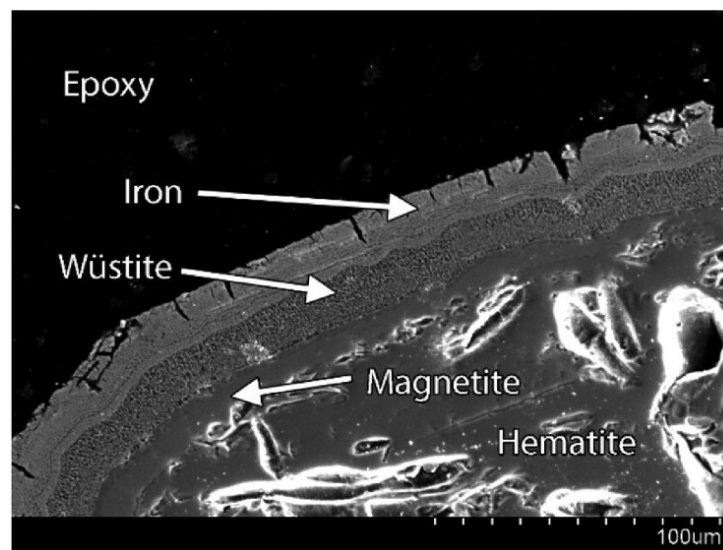


Figure 7. SEM photograph capturing Fe phases during hydrogen reduction Adapted from Ref. [34].

Chen Z. et al. conducted experiments on the reduction of hematite using hydrogen at various temperatures and observed that at temperatures above 900 °C, the reaction rate might actually decrease. This reduction is due to sintering effects and the formation of a dense outer layer on the surface of the iron ore, which can inhibit further reaction [38,63]. Similarly, He et al. recommend a maximum reduction temperature of 1000 °C when using pure hematite and hydrogen as the reducing gas, to avoid the drawbacks associated with sintering phenomena [63,80].

In the reduction in iron oxides using hydrogen, understanding the intricate balance between thermodynamics and kinetics is essential for optimizing the process. Thermodynamically, the stability of different iron oxide phases is heavily influenced by temperature changes. Higher temperatures are favorable for hydrogen as the reducing agent, as demonstrated by the expansion of the stable iron zone in the Baur–Glässner diagram (Figure 3). This creates a more favorable thermodynamic environment for hydrogen to effectively reduce iron oxides. Initially, the reduction reactions, such as converting hematite to magnetite, are slightly exothermic, which releases heat and reduces the need for external energy. As the process advances to reducing magnetite to wüstite and eventually to metallic iron above 570 °C, it transitions to being endothermic, requiring additional energy input. Kinetically, the reduction starts quickly with hydrogen gas adsorbing onto the iron oxide surface, efficiently initiating the reduction from hematite to magnetite. This phase is marked by high reaction rates due to the small size and high diffusivity of hydrogen molecules, which allow them to rapidly penetrate the iron oxide layers. As the reaction advances and denser iron layers form, the rate of reduction significantly slows. This slowdown is caused by the increasing challenge for hydrogen to diffuse through the denser metallic iron layers formed, particularly as temperatures increase and sintering begins. Sintering can further hinder kinetics by decreasing the material's porosity and surface area. Thus, effectively integrating thermodynamics and kinetics involves managing the heat to maintain thermodynamic favorability, while simultaneously overcoming kinetic barriers due to physical changes in the material's structure. Key strategies include maintaining optimal temperatures to support endothermic reactions while avoiding excessive sintering and optimizing gas flow and composition to counteract the effects of reduced diffusion in denser materials. This careful management ensures that hydrogen reduction in iron oxides remains efficient throughout the process.

2.2.3. Influence of Gas Flow on the Reduction in Fe Oxides by Hydrogen

In laboratory experiments, researchers have specifically studied the influence of hydrogen flow rates on the reduction process. Kulia et al. explored the impact of various

hydrogen flow rates (0.1, 0.2, 0.3, 0.4, and 0.5 L/min) on the reduction in magnetite ore at 900 °C and 1 atm pressure. Their findings indicated that increasing the hydrogen flow from 0.1 to 0.4 L/min enhanced the degree of reduction, as shown in Figure 8. However, flow rates above 0.4 L/min did not significantly improve the reduction outcomes, leading to the determination that 0.4 L/min is the optimal hydrogen flow rate for this process [44]. Kang et al. noted that there is a critical point at which changes in the flow rate of the reducing gas primarily affect the concentration of the gas at the reaction interface. Once the hydrogen flow rate exceeds this critical threshold, it indirectly influences the reaction rate by modulating the hydrogen concentration at the interface. Consequently, any further increase in flow rate beyond this point does not enhance the degree of reduction, indicating that the relationship between flow rate and reduction efficiency is not linear [81].

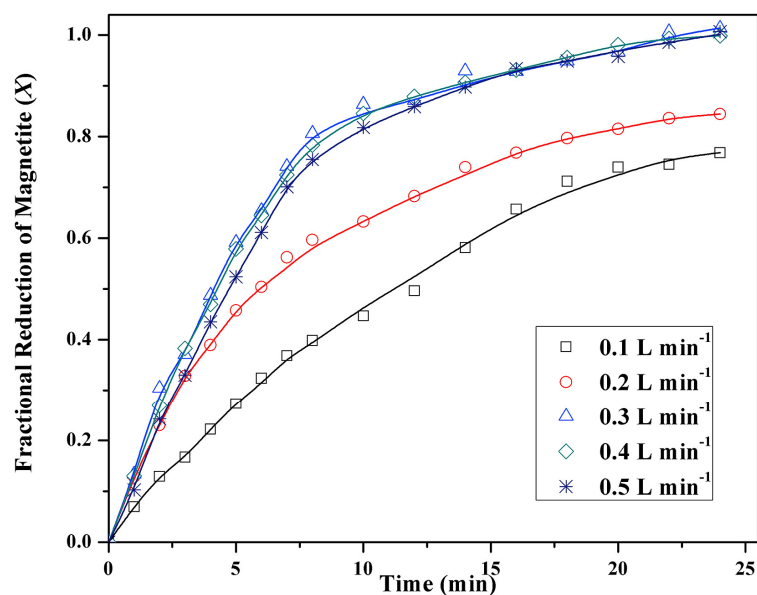


Figure 8. Graph of reduction of magnetite ore at different flow rates at 900 °C. Reprinted with permission from ref. [44]. 2024 Elsevier.

Peyiu Li et al. conducted research to evaluate the impact of gas flow rates on the reduction in magnetite to metallic iron at 570 °C. Their study found that when the gas flow rate was increased from 400 to 800 mL/min, the conversion degree (α) at the same reduction time saw a substantial increase. This suggested that the reaction rate was accelerating, and the external diffusion limitations typically associated with the fluidized bed were being mitigated. Further increase in the flow rate to between 800 and 1200 mL/min did not significantly affect the conversion degree, indicating a plateau in the influence of gas flow on the reduction efficiency. Based on these findings, the optimal gas flow rate to eliminate external diffusion issues and maintain a stable bubbling fluidized state in the bed was determined to be 1000 mL/min [54]. This optimal rate helps to ensure efficient contact between hydrogen and iron oxide particles, thereby enhancing the reduction process while preventing the inefficiencies associated with excessive gas flow.

As the gas flow rate increases, the concentrations of reducing gases and the gas velocity increase. Consequently, the Reynolds number, as well as the heat and mass transfer coefficients, are increased. An increase in the mass transfer coefficient between the bulk gas and the pellet surface leads to a higher concentration of reducing gases on the pellet surface, which diminishes the impact of mass transfer on the overall reaction rate. Similarly, with an increased heat transfer coefficient, the temperature of the solids rises, which leads to an increase in the reaction rate and solid conversion [82].

The Reynolds and Sherwood numbers are dimensionless numbers used in fluid dynamics and mass transfer analysis, respectively. They are important for characterizing different flow and transfer regimes in various systems.

Thomas Wolfinger's study focuses on the mathematical evaluation of iron ore ultra-fines for their use in a novel hydrogen-based fluidized bed direct reduction process. Typical samples of iron ore ultra-fines, such as pellet feed, are analyzed and classified for use in a fluidized bed. The operating field for a hydrogen-based fluidized bed direct reduction process using iron ore ultra-fines is depicted in the fluidized state diagram according to Reh's approach, and is compared to other processes [83].

Reh's diagram is used to classify different reactor types according to the material and gas properties and process conditions, for example, shaft reactors or circulating fluidized beds. The extended Reh diagram is crucial for optimizing the fluidized bed direct reduction process using iron ore ultra-fines. The diagram helps assess how variations in particle size impact fluidization quality and the minimum fluidization velocity, crucial for preventing excessive particle aggregation. It incorporates the effects of gas dynamics, such as type and flow rate, on gas-particle interactions through parameters like the Archimedes number and Reynolds number. This understanding is vital for controlling the reduction kinetics and ensuring efficient hydrogen contact with iron ore particles. The Reh diagram characterizes fluidization regimes, identifying operational limits to maintain stable fluidization despite the challenges posed by the fine nature of ultra-fines [83].

Geldart classified the fluidization behavior of solid powder materials into four groups within a plot of density difference between the particles and the fluidizing medium against the mean particle size d_p . Group A particles are fine and aeratable solids, which show high bed expansion and good fluidization quality. Group B particles are intermediate-sized particles that show little bed expansion, and bubbles appear when fluidization begins. Group C particles are very fine, and cohesive materials that form channels and agglomerates and are difficult to fluidize. Group D particles are coarse and large solids that form vertical channels [83].

Figure 9 displays an extended version of the Reh diagram, which includes various gas–solid reactor systems (fields a to e), the FINMET operating field, and the operating field R for the reduction of iron ore ultra-fines in a fluidized bed. The operating field R is described as follows:

- Particle diameters, d_p , in size range of 2 to 90 μm , to account for 95 wt.%.
- Densities of the ore and DRI, ρ_p , between 5000 and 3500 kg/m^3 .
- Gas densities, ρ_f , and dynamic viscosities, η_f , for the H_2 and $\text{H}_2/\text{H}_2\text{O}$ mixtures at temperatures of 873 to 1123 K and a pressure of 0.1 bar.
- Superficial gas velocity, u , between 0.15 and 0.30 m/s [83].

According to Geldart's and Goossens's classification, iron ore ultra-fines are mainly Group A, Group A/C, and Group C materials under ambient conditions and air. For the hydrogen-based reduction at higher temperatures, iron ore ultra-fines are mostly Group A/C and Group C, according to Goossens's classification. The operating field for iron ore ultra-fines requires an extended version of the Reh diagram and does not fall within the typical fields of circulating or bubbling fluidized beds. Changing process conditions such as temperature and gas properties has little impact on the fluidization conditions or the minimum fluidization velocity. However, altering the characteristic diameter due to sticking significantly affects both the fluidization conditions and the minimum fluidization velocity. Therefore, the characteristic particle or agglomerate diameter is the most critical parameter for ensuring a stable fluidized bed direct reduction process [83].

In another study, they claim that as the velocity of the reducing gas (H_2) increased from 2.3 cm/s to 6.2 cm/s , the Reynolds number increased from 0.012 to 0.033, and the Sherwood number increased from 2.08 to 2.13. This increase in Reynolds and Sherwood numbers signifies an enhanced turbulent flow and improved convective transport of mass and heat. Consequently, the mass transfer coefficient, which reflects the effectiveness of mass transport between the gas phase and solid particles, rose from 41.5 cm/s to 44.5 cm/s . This increment suggests that more reactive gas is being transported to the surface of the iron oxide particles efficiently, thereby increasing the surface reaction rate [84].

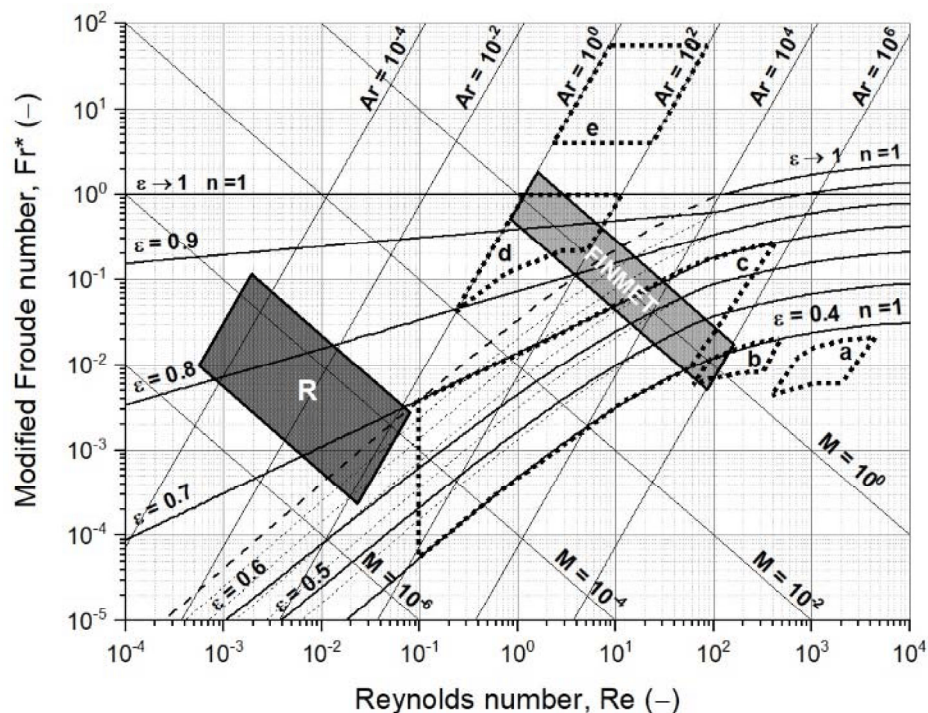


Figure 9. Extended version of the fluidized state diagram following Reh's approach, (a) shaft furnace, (b) moving bed, (c) particulate and bubbling fluidized bed, (d) circulating fluidized bed, (e) pneumatic transport reactor, (FINMET) operating field of FINMET® according to Schenk, and (R) operating field, Fr^* —modified Froude number is defined by the ratio between the inertia force and the weight force Adapted from Ref. [83].

The higher gas flow rates induce greater turbulence which disrupts the boundary layers around the particles more effectively, enhancing both mass and heat transfer. This results in a higher overall rate of reduction reaction, as observed from the doubling of the reduction rate at a gas velocity of 6.2 cm/s. In fluidized beds, although it is usually assumed that the gas flow in excess of the minimum fluidization velocity does not affect the mass-transfer coefficient in the dense phase significantly, the study findings suggest an additional transfer mechanism at play [84].

This mechanism can be attributed to enhanced transfer between the gas in the dense phase of the bed and the solid particles. Despite the beds being under chemical control, where the reaction rate should theoretically remain unaffected by changes in gas velocity, the actual impact on the overall rate and solid conversion demonstrates that fluid dynamics and enhanced mass and heat transfer efficiencies contribute significantly to the efficiency of the reduction process in fluidized beds. This complexity underscores the dynamic nature of fluidized bed operations and the critical role of gas flow rates in optimizing process outcomes [84].

2.2.4. Influence of the Composition of the Reduced Material on the Reduction in Fe Oxides by Hydrogen

The influence of the composition of the reduced materials was examined by Edstrom et al., who compared the hydrogen reduction of hematite and magnetite. As illustrated in Figure 10, the reduction of hematite by hydrogen occurs faster than that of magnetite, particularly at higher temperatures. This difference is attributed to the hard and dense shell of magnetite, which impedes diffusivity [67]. Additionally, the higher density of hematite (5.260 g/cm³) compared to magnetite (5.175 g/cm³) means that the reduction in hematite to magnetite involves volume changes that lead to microcracking. These cracks act as pores and enhance gas diffusion [67].

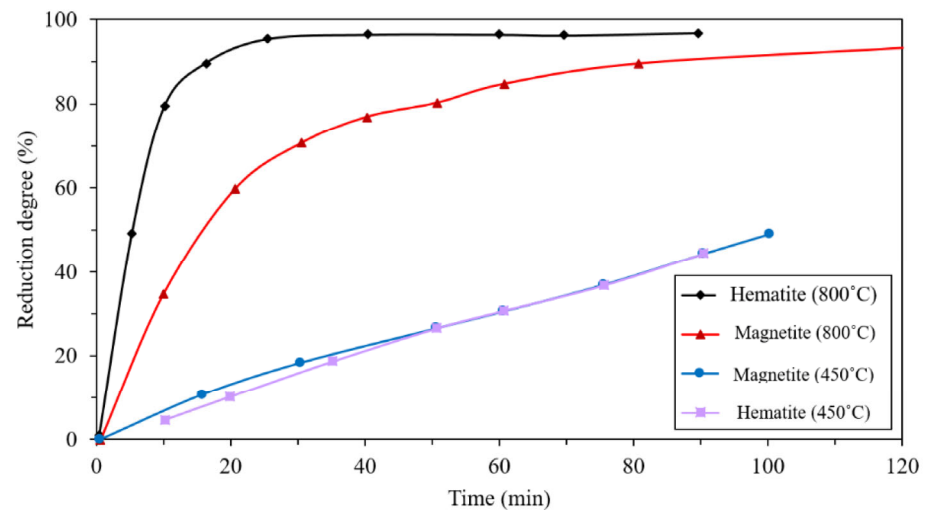


Figure 10. Comparison of the reduction of hematite and magnetite at two temperatures: 450 °C and 800 °C Adapted from Ref. [67].

Heikkilä et al. compared the reduction behavior of iron ore pellets, agglomerates, and lump ore at various temperatures. The lump ore exhibited the lowest reduction rate at all temperatures, attributed to its low porosity and surface area. At temperatures below 800 °C, the pellets reacted more quickly, but at higher temperatures, the rate of agglomerate reduction was greater (as shown in Figure 11). This is due to the higher initial content of magnetite in the agglomerates, which reduces more slowly at lower temperatures [85].

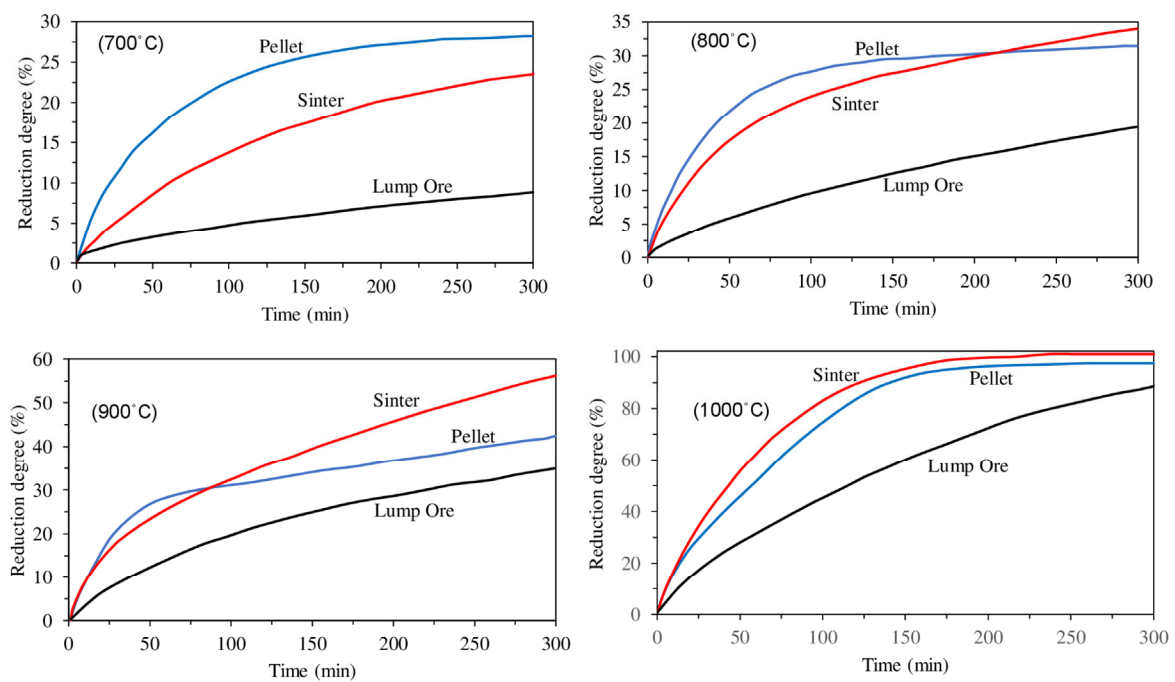


Figure 11. Degree of reduction as a function of time for iron ore pellet, agglomerate and lump ore at 700, 800, 900 and 1000 °C Adapted from Ref. [85].

Hou et al. investigated the effect of particle size on reduction by studying particles ranging from 0.025 to 0.2 mm. Their findings indicated that for particle sizes smaller than 0.045 mm, the reduction rate's dependence on particle size is not significant. This is because for particle sizes below 0.045 mm, the internal diffusion resistance becomes negligible [86].

Yingxia Qu et al. also studied the effect of particle size on the reduction in fine-grained hematite particles. They concluded that particle size has a negligible impact on the degree of reduction [46].

Considering that different iron (Fe) materials were used in various studies, each with different chemical and mineralogical compositions, deviations in the reduction results can be linked to these differences in composition and the purity of the input materials. A greater impact of the input Fe materials on their hydrogen reduction is observed with commercial iron ores and pellets, where impurities are present in larger quantities (typically 5–15%). In these materials, the influence of individual oxides such as SiO_2 , CaO , MgO , and Al_2O_3 on hydrogen reduction becomes evident.

Richard Sundberg, in his master's thesis, investigated the effect that gangue has on the reduction rate of iron oxides. The impact of gangue on the reduction of iron oxides depends on the type and amount of oxides present. Oxides typically include SiO_2 , CaO , MgO , and Al_2O_3 . Al_2O_3 can increase the reduction rate if its content is less than 3%. Normally, when magnetite is reduced, dense iron layers can form, which simultaneously prevent the reducing gases from diffusing through to the core of the pellet. If Al_2O_3 is present, it can at least partially hinder the formation of these dense iron layers, maintaining the overall reduction rate. Some amount of CaO may also increase the reduction rate, while MgO lowers it. The addition of SiO_2 may lead to the formation of iron silicate (fayalite) during reduction. The presence of fayalite has a detrimental effect on the reduction rate, particularly during the later stages of reduction (from wüstite to iron). This negative impact is more pronounced when the reductant is CO as opposed to H_2 . Most reviewed studies reported a beneficial effect of CaO on the reduction rate. Some mechanisms by which CaO accelerates reduction include increasing the initial porosity, dissociating wüstite, and promoting a porous structure in the reduced iron layer. The positive impact of Al_2O_3 addition on the reduction rate can be attributed to the formation of hercynite precipitates, which are proposed to facilitate gas diffusion by disrupting the atomic arrangement within the iron oxide structure. The effect of MgO on the reduction in iron oxides can be either beneficial or deleterious, depending on the phases formed during reduction. The incorporation of MgO into magnetite appears to facilitate the formation of magnesio spinels, thereby promoting a porous structure. However, when MgO is added to wüstite compacts, a dense structure is formed due to the formation of magnesio-wüstite [87].

Heidari et al. in their review, mentioned that by increasing the temperature and hydrogen concentration, the formation of the phases, such as MgFe_2O_4 and $\text{Fe}_x\text{Si}_y\text{O}_4$, become faster, which increases the resistance of interfacial chemical reaction during the reduction. Higher contents of CaO , SiO_2 , and MgO can be found in larger particles, which leads to the formation of cracks and accelerate the reduction of wüstite [67].

2.2.5. Influence of Pressure on the Reduction in Fe Oxides by Hydrogen

Technologies for direct reduction, such as shaft furnaces (examples include MIDREX and HYL Energiron) and fluidized beds (like FINMET and CIRCORED), have been developed and are currently widely used in the industry. The latest version of the MIDREX process operates at a pressure slightly above normal atmospheric levels, approximately 1.5 to 2.0 bar. In contrast, the HYL Energiron process functions at a much higher pressure, over 5 bar. Fluidized bed reactors, used in these contexts, operate at pressures above 4 bar, which is necessary to fluidize ore fines. It is crucial to understand how gas pressure influences the reaction in HDR processes [88].

A few studies have evaluated the impact of gas pressure on HDR processes using pure reducing gases (H_2 or CO) or gas mixtures, which include H_2 , CO , H_2O , CO_2 , and inert gases [69,89–91]. These investigations highlighted the nuanced impact of the absolute pressure of the gas mixture, within a range of 1 to 3 bar, on the kinetics of the reduction process [69,92]. In contrast, an increase in the partial pressure of reducing gases (H_2 or CO) has been found to effectively enhance the reduction kinetics [90].

Nevertheless, it is the partial pressure of the reducing gases that more significantly influences the reaction's driving force than the absolute pressure. A higher partial pressure of these gases indicates a greater number of moles of the reducing gas within a given volume of the reaction chamber. This increase improves the likelihood of gas molecule dissociation and the frequency of collisions between the reducing gas molecules and iron oxides, thereby substantially enhancing the reaction process. Specifically, when pure H₂ was used, an increase in absolute pressure (ranging from 5 to 36 bar) facilitated rapid reduction kinetics [89]. From a thermodynamic perspective, this effect can be attributed to an increase in the partial pressure of H₂, as the quantity of hydrogen gas significantly increases in the reactor (which has a fixed volume), while the amount of H₂O remains relatively constant [89].

Habermann et al. [90] investigated the impact of total pressure on the reduction rate of hematite using reducing gases with high hydrogen content in a fluidized bed reactor, maintaining a constant superficial gas velocity. They found that, at a constant partial pressure of hydrogen in the reducing gas (constant molar flow), an increase in total pressure does not enhance the reduction rate during the early and medium stages of the process. However, at the final stage of reduction, the slowdown in the reduction rate can be delayed to achieve higher degrees of conversion by using higher pressures. Additionally, with increasing total pressure while keeping the partial pressure of hydrogen constant (resulting in a higher molar flow), an increase in the reduction rate was observed [92].

However, the literature reveals a scarcity of comprehensive studies on how pressure impacts the HDR process. Given the presence of multiple factors that control the rate, including gaseous diffusion, chemical reactions, solid-state diffusion, and others, it is important to gain a clearer understanding and separation of the effects of pressure on different reduction processes and reactor conditions [88].

Understanding the specific impact of pressure on the hydrogen direct reduction (HDR) process is complex, due to the interrelated dynamics of gaseous diffusion, chemical reactions, and solid-state diffusion involved in the process. Hydrogen gas diffusion through the iron ore matrix is crucial for determining the rate of reduction reactions. The pressure affects the hydrogen diffusion coefficient in the gas phase, influencing how effectively hydrogen can infiltrate the deeper regions of iron ore pellets or lumps. Pressure not only influences the speed at which hydrogen moves, but also directly impacts the chemical reaction kinetics of converting iron oxides into metallic iron. Generally, an increase in pressure raises the partial pressure of hydrogen, which may accelerate the reduction reactions. However, this relationship is not straightforward, as it varies based on the specific kinetics and thermodynamics at different pressures. Once hydrogen reaches the ore's interior, it must move through the solid structure of the iron oxides to react at specific sites. The impact of pressure on this type of diffusion can be complex and is often affected by the ore's microstructure, such as its porosity and the presence of crystal defects. Moreover, the physical characteristics of the iron ore, including its porosity and permeability, play a significant role in how gases diffuse through the material. Increased pressure might compact the material, potentially reducing its permeability and offsetting the advantages of enhanced diffusion from higher pressure. Impurities and gangue materials within the ore can also alter the reduction kinetics, with their behavior potentially changing under different pressure conditions, adding another layer of complexity to isolating the effects of pressure on the reduction process. Precisely controlling and measuring pressure in the high-temperature conditions typical of HDR processes poses a technical challenge. Consistent application of uniform pressure and maintaining stable experimental conditions across tests are difficult. Accurately determining the rate of hydrogen consumption, measuring diffusion rates, and tracking reduction progress under high pressures and temperatures are significantly challenging. These measurements require advanced sensing and imaging technologies, which, despite their capabilities, may be limited by the demanding conditions of HDR processes [69,88–92].

2.3. Results of Research Studies Focused on the Reduction in Iron Pellets with Hydrogen

Authors in international publications have extensively researched the reduction in iron pellets with hydrogen. Consistent with findings related to the reduction in ores and synthetic powders, the highest rate of reduction was observed when using H₂, while the lowest rate was achieved with CO. The reduction rate with a gaseous mixture of H₂ and CO was intermediate [51,93]. Qing Lyu et al., who studied the reduction of industrial pellets in a CO:H₂:N₂ atmosphere at various ratios, found that increasing the temperature from 700 °C to 1000 °C significantly accelerated the reduction process [38]. They also examined the composition of the reducing gas. At 700 °C, the degree of reduction reached 87.32% after 2.5 h in a gas mixture containing 30% CO + 20% H₂, compared to only 60.41% with a mixture of 30% CO + 5% H₂ [59].

During the reduction of iron ore pellets, the internal structural changes—specifically porosity and grain morphology—are critical factors that influence both the efficiency of the reduction process and the quality of the resulting iron product. These factors vary significantly with temperature changes during the reduction. Here is how each factor plays a role [94].

Porosity is crucial for allowing reducing gases, like carbon monoxide (CO) and hydrogen (H₂), to penetrate the pellets and react with the iron oxides [94,95]. Porosity is a crucial factor limiting the rate of the reduction process. It is influenced by the pellet's porosity in terms of size, distribution, and tortuosity of pores, which affect the volume of hydrogen reacting with the internal surface of the pellet. When porosity is low and pores on the surface are small, hydrogen diffusion into the pellet becomes hindered, making solid-state diffusion from the surface more critical, and much slower [96]. Higher porosity facilitates better gas diffusion, leading to more efficient reduction. Increased porosity typically enhances the surface area available for chemical reactions, thus increasing the rate at which reduction can occur. During the initial stages of heating, the thermal decomposition of certain compounds (like carbonates) within the pellets can increase porosity. At higher temperatures, sintering effects can reduce porosity as grain boundaries begin to fuse, potentially limiting gas access to the pellet's core and slowing down the reduction process [94,95].

At higher temperatures, the grains within the pellets can grow larger. While this can potentially strengthen the pellet structure post-reduction, it may also reduce porosity as the grains merge. Different temperatures can lead to phase changes in the iron oxides (e.g., from magnetite to wüstite to metallic iron), each with distinct grain morphologies which can affect the mechanical properties of the pellets. Larger, well-formed grains can enhance the mechanical integrity of the pellets, making them less prone to degradation during handling and transport. Optimizing the temperature profile during reduction is essential to balance the processes of porosity generation and grain growth. Effective temperature management can maximize reduction efficiency while maintaining the structural integrity of the pellets [94,95].

The reduction is highest for pellets with the highest porosity [40]. At elevated temperatures, the reduction process is accelerated in a reducing atmosphere. An increase in the porosity of the pellets also occurs in the reduction process itself [97]. The total porosity increases at higher temperatures, while the porosity inside the reduced iron decreases and the porosity between the particles increases [58,98].

The kinetics of reduction depends on the starting pellets properties [97]. The reduction time is primarily influenced by pellet diameter, related to pellet density and the reducing atmosphere. Changes in pellet diameter affect how density influences the reduction; higher density diminishes the impact of diameter, whereas in larger, less dense pellets, the effect of density is less pronounced. Reduction time also correlates with both the absolute porosity and the dimensions of surface pores—larger pores facilitate faster reduction [96].

Pasquale Cavaliere et al. investigated that the time to 95% reduction is mainly influenced by the pellet's diameter and density and then by the reduction temperature. The rate of reduction in the first stages is mainly influenced by the reduction temperature and then by the pellet's physical properties [97].

In general, as the pellet diameter increases, the reduction rate decreases [99]. Metolina P. et al. confirmed that the increase in temperature and decrease in pellet size considerably favor the reduction rate [100].

Yan Ma et al. highlighted the significant impact of pellet microstructure on reduction efficiency, with heterogeneity in metallization rates observed along the pellet radius during the reduction process at 900 °C. The surface showed high metallization while deeper layers contained substantial amounts of unreduced wüstite. This heterogeneity was attributed to delayed oxygen diffusion in these areas, emphasizing the importance of microstructural control for efficient reduction. Microtomography revealed increasing porosity and pore tortuosity as reduction advanced, with these structural changes contributing to slower kinetics in later stages. SEM analysis indicated that the initial reduction stages led to a porous structure with many small grains, but as reduction proceeded, the structure densified, particularly in the outer layers, hindering further gas diffusion [101].

Ming-Hua et al. studied direct reduction behavior and dynamic characteristics of oxidized pellets under the 75% H₂–25% N₂ atmosphere at 760, 900, and 1000 °C. It is observed that the section surface becomes brighter after reduction under higher temperature, which attributes to the reflective performance enhancement with the increasing metallic content. Pellets reduced at 760 °C are characterized by a dark unreacted core (5 mm in diameter) surrounded by the light iron layer, which means the reduction has not been completed. Pellets reduced at 900 and 1000 °C were uniform and bright. Optical microstructures of pellets reduced at 760 °C showed lots of metallic iron in bulk in the exterior, while a large amount of wüstite, which looks darker than iron, exists mainly in the interior and the metallic iron is scattered in the wüstite. It is obvious that the content of iron decreases gradually from the outside in. Microstructures of pellets reduced at 900 and 1000 °C showed that there is no significant difference in the microstructures between the edges and the interior. The uniform distribution of massive metallic iron is found all across the visual field. It is noted that more pores and smaller iron grains are observed. The reduction degree increases significantly from 0.746 to 0.919 when temperature increases from 760 °C to 900 °C. The value further increases to 0.989 at 1000 °C, which is in line with microstructure observation that more pores found at 1000 °C may facilitate the diffusion of reduction gas through the production layer and reaction with wüstite at the later stages, leading to the reduction enhancement [102].

Kovtun et al. examined that during pellet reduction, iron oxide presence varied with temperature. At 700 °C and 800 °C, iron oxide (likely FeO and/or Fe₃O₄) was observed, with it being more concentrated at the pellet edges at 800 °C. By 900 °C and 1000 °C, no iron oxide was detected, indicating better reducibility at higher temperatures. Initially, fine micropores and dense metallized iron formations were seen at 700 °C and 800 °C, with larger micropores at 800 °C. Macropores were absent at these lower temperatures, but appeared at 900 °C and 1000 °C, suggesting enhanced hydrogen diffusivity and increased reduction rates. Surface cracks at 1000 °C also indicated high hydrogen diffusivity and effective reduction [103].

Patisson et al., in their review study, focused on scanning electron microscopy observations of the internal structure of pellets during reduction with hydrogen, as shown in Figure 12. Initially, a pellet is a porous agglomerate of dense hematite grains (f). After reduction, the overall structure of the pellet remains largely unchanged, except for a slight increase in porosity. However, significant transformations occur at the grain scale. The iron grains (a–e) are markedly different from the initial hematite grains, and their metamorphosis varies with temperature; iron grains formed at higher temperatures are larger and smoother. The center column (f–j) illustrates the transformation over time. Initially, some pores appear on the surface of the grains (g–h). As reduction progresses to the wüstite stage, the grains begin to fragment into smaller pieces, referred to as crystallites (i). Subsequently, the iron phase expands internally at the expense of the diminishing wüstite cores within the crystallites (k–n). At temperatures above 900 °C, the iron spreads across the crystallites and tends to amalgamate them [104].

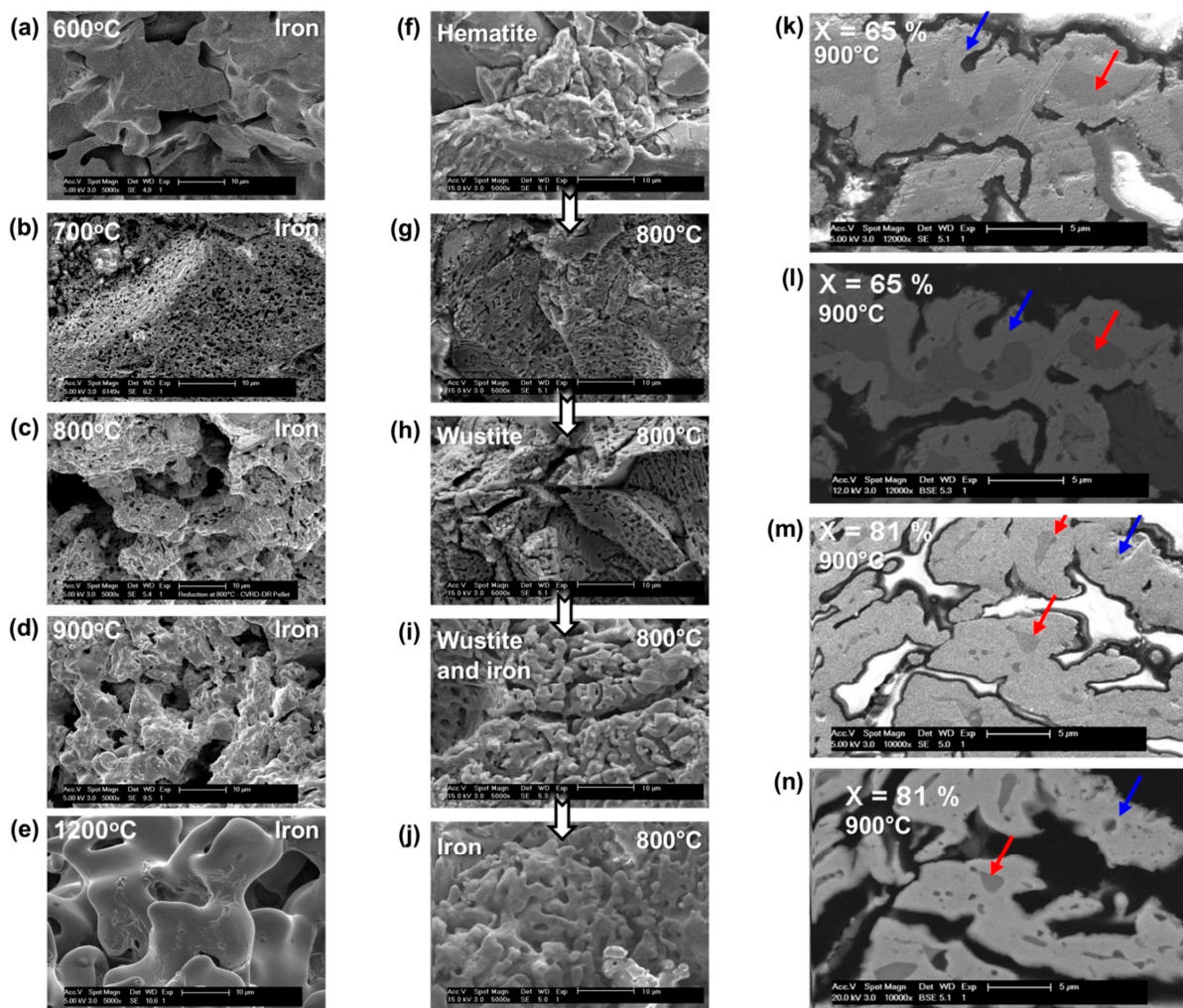


Figure 12. SEM micrographs showing the morphological changes at the granular scale in CVRD-DR pellets; (a–e): iron grains after reduction at different temperatures; (f–j): grains in different stages of a reduction at 800 °C; (k–n): polished cross-sections at conversion degrees of 65% (k,l) and 81% (m,n) for samples reduced at 900 °C; the red arrows point to shrinking wüstite cores (dark gray) surrounded with a spreading layer of iron (light gray), indicated by the blue arrows. Adapted from Ref. [104].

The structural changes impact not just the speed of reduction, but also the properties of the iron produced. Understanding and controlling the internal structural changes of iron ore pellets—specifically porosity and grain morphology—throughout the reduction process at varying temperatures is key to enhancing both the efficiency of the reduction process and the quality of the final iron product. This includes carefully managing the thermal profile during reduction to optimize these structural features [94,95].

The Reduction Swelling Index (RSI) quantifies the increase in pellet volume during reduction and is known to rise with increasing temperature [58,105,106]. Scharm et al. found that the RSI is significantly higher in an H₂ atmosphere compared to a CO atmosphere, peaking during the first stage of reduction (Figure 13) [58]. Conversely, Yi et al. noted that pellet swelling intensifies with both increasing temperature and CO content in the atmosphere [107]. The expansion in CO atmospheres is often maintained in later stages due to the formation of iron whiskers. The increase in pellet volume is primarily attributed to the formation of the FeO phase, which causes swelling. However, in an H₂ atmosphere, pellets rapidly transition through the FeO phase, which reduces subsequent swelling [107]. Zhao et al. observed that the RSI of pellets decreases with increasing H₂

content; they also noted that temperature has a more significant impact on swelling than the composition of the reducing atmosphere [105]. Kovtun et al. found that the chemical composition and porosity of pellets significantly affect the RSI; specifically, pellets with lower gangue (CaO and SiO_2) content exhibited higher RSI at the same temperature [106]. Conversely, Sharma et al. reported that an increase in gangue content leads to a decrease in RSI [108]. Nyankson et al. observed that pellets reduced with 100% H_2 developed larger and more visible cracks compared to those reduced with 100% CO , suggesting that the extensive swelling in H_2 atmospheres may contribute to these formations [37].

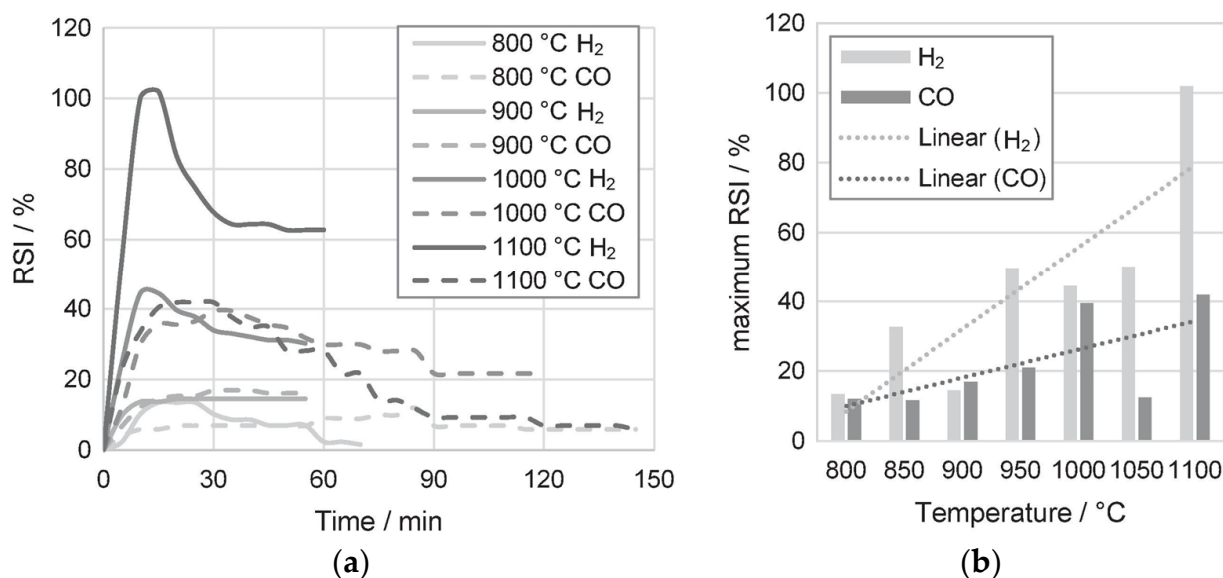


Figure 13. Reduction swelling index (RSI): (a) of individual pellets during their reduction in an atmosphere of H_2 and CO at 800, 900, 1000, and 1100 °C; (b) comparison of the maximum RSI of all individual pellets reduced in an atmosphere of H_2 and CO at each temperature. Reprinted with permission from ref. [58]. 2024 Elsevier.

2.4. Results of Research Studies Focused on the Reduction in Iron Materials with Hydrogen Using Hydrogen Plasma

The reduction potential of Fe materials using hydrogen plasma was confirmed through various studies [109,110]. Isnaldi R. Souza Filho et al. investigated what they termed hybrid reduction of hematite pellets, which combines two processes: DR (Direct Reduction in a hydrogen atmosphere within furnace equipment) and HPR (Hydrogen Plasma Reduction), as illustrated in Figure 14 [111]. They found that the maximum utilization and greatest potential for H_2 savings occurred when the hematite pellets were initially reduced by 38% at 700 °C in an H_2 atmosphere and then further reduced to liquid iron in a plasma furnace using an Ar-10% H_2 mixture (Figure 14).

Overall, reduction occurs faster using hydrogen plasma (or a combination of the Direct Reduction (DR) process and hydrogen plasma) than using the DR process alone. The complete transformation of hematite into liquid iron is achieved after only 15 min of exposure to hydrogen plasma. In contrast, in the DR process, sponge iron is produced within approximately 70 min at 700 °C and about 40 min at 900 °C when directly exposing hematite to H_2 . Moreover, arc plasma operates much more stably when processing semi-reduced oxides (for example, pellets reduced by 38%) compared to using hematite-based materials as the starting input [111].

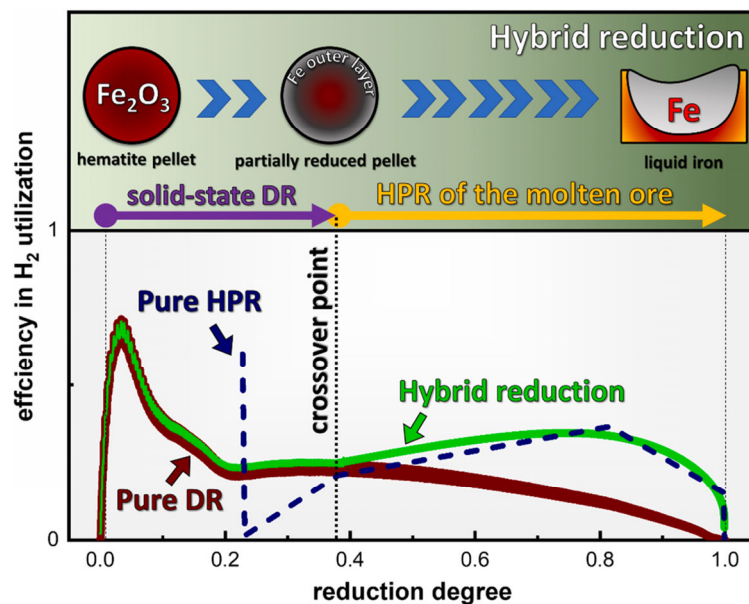


Figure 14. Overall efficiency trend in hydrogen consumption during the DR process (represented by the burgundy line), hydrogen plasma-HPR process (blue dashed line) and for hybrid reduction (green line). Reprinted with permission from ref. [111]. 2024 Elsevier.

2.5. Critical Analysis of Reduction in Iron Oxides with Hydrogen, Advantages and Disadvantages of Reduction of Iron Oxides with Hydrogen

The critical point in the reduction of Fe materials using hydrogen primarily focuses on achieving conditions where the reaction is thermodynamically favorable and can proceed efficiently. This involves maintaining a high temperature, typically around 800 °C, necessary to effectively drive the reduction reaction. At these temperatures, the thermodynamic conditions allow hydrogen to reduce iron oxides into metallic iron, simultaneously producing water vapor as a byproduct. Additionally, managing the hydrogen pressure is crucial, as higher pressures can enhance the reduction rate due to the increased availability of hydrogen molecules to react with the iron oxides. Moreover, the kinetics of the reaction are significantly influenced by the physical characteristics of the iron oxide, such as particle size, porosity, and the specific oxide form (hematite, magnetite, etc.). It is essential to optimally control these parameters—temperature, hydrogen pressure, and material characteristics—to ensure an efficient reduction process in an industrial setting. This includes meticulously managing the reaction environment to prevent the reoxidation of the reduced iron by controlling the gas composition, particularly the ratio of hydrogen to water vapor produced in the reaction.

The reduction in iron oxides by hydrogen is a topic that has been extensively investigated in numerous studies. However, uncertainties still exist regarding the details of the process. One area of uncertainty is the effect of changes in the composition of the H₂-H₂O gas mixture, which impacts the kinetics of the reduction process. Research has shown that this reaction positively influences the reduction rate at lower temperatures, but has almost no noticeable effect at higher temperatures. While there has been considerable research into the thermodynamics and kinetics of reducing iron oxide using CO, H₂, and their mixtures to enhance understanding of the reduction mechanisms, there is a critical need to further explore the interactions between CO (and CO₂) and H₂ (and H₂O) across a wide range of temperatures. This will help identify the most effective H₂ concentration for the reduction process. The kinetics of hydrogen reduction in iron oxides continues to be a subject of research; the effects of changing gas composition and other reaction conditions such as reducing gas flow, pressure, and temperature remain not fully understood.

All research so far has concluded that the kinetics of the reduction in iron oxides by hydrogen are faster at higher temperatures (up to approximately 1000 °C). Increasing

the temperature further might accelerate the reduction rate; however, depending on the mineralogical composition of the Fe ores or pellets, higher temperatures might lead to the melting of the iron oxides, potentially slowing down the reduction process significantly. Parameters such as temperature, particle diameter, and particle porosity significantly impact the reduction reactions. The reduction in wüstite to iron is the slowest stage since this step involves removing most of the oxygen from the ore, and the bond between oxygen and iron is the strongest in this phase. Several models for reducing iron oxides by hydrogen have been developed in research studies. Comparisons between these models and experimental results indicate that, while the models can provide fairly accurate outcomes, some parameters might not be correctly estimated. This discrepancy is partly due to the complex nature of the experimental conditions which involve numerous variables that need to be considered. Therefore, accurately determining these parameters from limited experimental data is challenging, and the influence of certain parameters (e.g., temperature, flow, pressure, and physicochemical state of the particle) is highly interdependent. To improve modeling and parameter prediction, a comprehensive set of experimental data should be used to more precisely study the kinetics. Additionally, it would be beneficial to explore the chemical kinetics of hydrogen reduction of iron oxides at very small particle sizes to minimize the overlapping effects of chemical reaction rate, mass transfer, and diffusion. In the direct reduction in Fe materials with hydrogen, the following main steps should be examined more thoroughly:

- mass transfer of the hydrogen from the stream to the surface of the reduced material;
- diffusion of the approaching gas through the thick film surrounding the reduced material;
- diffusion inside the surface pores;
- adsorption of hydrogen at the different oxides interphases;
- consequent oxygen removal through phase boundary reactions;
- formation of water vapor, iron oxides and ferrous iron;
- desorption of all the gases belonging to the reactions;
- solid state diffusion of the reacted products;
- diffusion of gaseous products back toward the surface;
- and mass transfer of the gaseous product toward the stream.

The development of thermodynamic models plays a crucial role in using computational methods to study the impacts of various variables on the chemical system of iron oxide reduction with hydrogen under equilibrium conditions. The aim is to derive the simplest possible model that can predict the output parameters—such as quantities, chemical and mineralogical composition, and total heat—based on the input chemical analysis of Fe materials. However, some thermodynamic models struggle to accurately predict the reaction mechanism of iron oxide reduction by hydrogen, as they do not always correlate well with the kinetic behaviors observed in experiments. The microstructure of metallized products, when reduced with hydrogen, significantly influences the outcomes. Phase transformations during hydrogen reductions can lead to complex developments in the microstructure of the metallized product. Various components of the microstructure play critical roles in facilitating the accelerated transport of reducing gases. One significant kinetic barrier is nucleation during phase transformations, particularly the slow process of iron formation. Research on this phenomenon is limited, but critical. Additionally, the size of the reduced particles has a profound effect on metallization and reduction with hydrogen. Initially, this factor was considered minor due to the rapid diffusion of hydrogen; however, the transport of oxygen and the removal of water vapor from the reaction zone present significant kinetic challenges and complications.

Consequently, a detailed investigation of the ideal sizes of Fe pellets or ores is an important area of research for optimizing the direct kinetics of hydrogen reduction and the metallization of iron oxides. Considering the physical changes that occur, the volume of the pellets expands during reduction, and significant swelling phenomena can lead to irregular reduction outcomes. This swelling can decrease the permeability of the pellets and, in some cases, cause the entire burden to collapse. Therefore, it is crucial to accurately characterize

the swelling behavior of the pellets before proceeding. Swelling typically occurs as wüstite converts into iron, a phase during which there is limited nucleation. The nuclei that do form tend to grow in a needle-like shape, leading to the volumetric expansion observed as swelling. This transformation also correlates with a decrease in the compression strength of the structure, making it prone to generating fines. In terms of industrial pellets, findings are often inconsistent, particularly concerning the detailed kinetics of pellet reduction under various temperatures and pressures. This inconsistency is largely due to the initial composition of the pellets, as well as their density, and the size and shape of their pores, all of which significantly affect the reduction process. As a result, there is no consensus on how all these factors influence the development of the process. This lack of agreement leads to numerous contradictions in existing research, partly because many studies focus exclusively on one type of pellet in terms of its composition and porosity. Another fundamental aspect affecting the direct reduction behavior is the material composition in terms of iron oxides, different metals oxides, gangue, and impurities. These components crucially impact the reduction dynamics and the quality of the final metallized product.

The kinetics of reduction reactions slow down in the case of ores with a higher impurity content. In the case of synthetic powders with a purity of 99.5% to 99.9%, the impacts of individual impurities on the reduction process have not yet been detailed in research studies. Studies indicate that pure synthetic powders are best reduced by hydrogen, achieving high degrees of reduction (approximately 95–99%). As shown in the study by Hessels et al. [61], even for highly pure iron oxides, the kinetics of reduction vary significantly due to the influence of macrostructure (particle size, porosity) and microstructure (crystal size, vacancies, impurities), as well as experimental conditions (temperature, time, methods). As a result, there is currently no generalized kinetic model or parameters for the reduction in iron oxide that consider deviations in reduction results due to differences in the composition and purity of synthetic powders. New types of synthetic powders therefore require their own kinetic measurement and analysis. Synthetic powders based on Fe oxides have unique properties, such as chemical and mineralogical composition, size, surface morphology, etc., for which results are available only for the specific materials used. In the future, it would be necessary to focus on creating more detailed mathematical models for the reduction of Fe oxides using hydrogen, which would take into account the current composition and purity of the Fe materials used for reduction.

The use of hydrogen in the reduction of Fe materials offers significant advantages beyond its low environmental impact, primarily due to its superior thermodynamic and kinetic properties. These properties enable the reduction process to be conducted at significantly lower temperatures and achieve a higher degree of reduction and metallization compared to traditional carbonaceous reducing agents. A key benefit of using hydrogen is the potential to produce a product with very low levels of impurities; this is because hydrogen, as a gas, does not introduce additional contaminants like solid carbonaceous materials might. Moreover, there is an urgent need to develop new ironmaking methods that move away from traditional blast furnaces and instead utilize hydrogen as the main reducing agent. This shift is driven by global concerns about climate change and the necessity to adopt more sustainable industrial practices. However, despite these innovations, steel remains indispensable globally due to its affordability and superior properties. The transition to more technologically advanced, yet environmentally friendly production methods must not compromise the safety, stability, efficiency, and cost-effectiveness of traditional processes. This is especially pertinent considering the production costs of hydrogen are currently prohibitively high. While incorporating hydrogen can accelerate the reduction process, producing hydrogen is energy-intensive and alters the thermodynamic characteristics of the reduction process due to endothermic reactions. As such, significant volumes and high pressures are necessary to mitigate heat losses. Another challenge is the high cost of produced hydrogen and the stringent safety measures required due to its highly flammable and explosive nature. Furthermore, existing research studies often overlook a thorough analysis of the risks associated with using hydrogen as a reducing

agent, which is a critical area that needs addressing to ensure the safe implementation of these new technologies.

To ensure hydrogen benefits metallurgy, its use must significantly expand, and its production must come from renewable energy sources (including nuclear) and be completely decarbonized. Widespread use of hydrogen as a reducing agent in the metallurgical industry also requires the availability of hydrogen infrastructure, transport, and efficient hydrogen storage technologies. Additionally, missing regulations on hydrogen application in metallurgical technologies and ensuring the safety of technological devices pose challenges. Currently, a significant barrier to adopting hydrogen as a reducing agent in the metallurgical industry is its production costs, which result in high prices for final products. Another issue is that different iron and steel production processes have varying hydrogen purity requirements. The blast furnace process does not require highly pure hydrogen, as it uses a hydrogen-rich mixed gas. In contrast, the DRI process typically uses a reducing gas with higher hydrogen content and purity, which is currently difficult to achieve with its majority production from fossil fuels. The use of hydrogen for ore reduction is also influenced by various technological and technical parameters (e.g., the quality of input material, the reducing device used, materials in contact with hydrogen, flue gas monitoring, etc.). Acquiring high-quality ore (or pellets) for efficient hydrogen reduction will continue to be challenging. Problems may also arise from low-temperature powdering of grains and sticking of the batch in reduction devices during hydrogen reduction. Given the endothermic nature of hydrogen reduction, maintaining furnace temperature is challenging and requires external heat supply, which can cause stability issues in the process [112,113].

3. Discussion

Laboratory research on the reduction in iron ore using hydrogen focuses on exploring the feasibility and effectiveness of using hydrogen as a reducing agent in metallurgical processes. Below are the key aspects of research regarding the use of hydrogen as a reducing agent in the reduction of iron (Fe) commodities:

- Kinetics of reduction: Researchers study the kinetics of hydrogen reduction reactions at the laboratory level. This involves examining the rate at which iron oxides (usually hematite or magnetite) are reduced to metallic iron in the presence of hydrogen.
- Optimum temperature and pressure: Identifying the optimal temperature and pressure that maximize the speed and completeness of the reduction process is a key area of research. Scientists are working to pinpoint these conditions.
- Mechanisms of reduction: Understanding the mechanisms in hydrogen reduction reactions is crucial. Researchers are identifying reaction pathways to better control and enhance the reduction process.
- Gas composition: Researchers experiment with different gas compositions, including variations in hydrogen concentration, to assess their effects on reduction efficiency. This may involve using pure hydrogen or a mixture of gases with a high hydrogen content.
- Material characterization: Before and after reduction, researchers use analytical techniques such as X-ray diffraction (XRD), scanning electron microscopy (SEM), and energy-dispersive X-ray spectroscopy (EDS) to characterize the iron ore and reduced products.
- Effect of impurities: The research explores the impact of impurities in iron ore and hydrogen gas on the reduction process and the quality of the obtained iron.
- Reaction Modeling: Mathematical modeling and simulations are employed to predict and optimize process parameters, providing insights into reaction behavior and guiding experimental design.
- Energy efficiency: The research aims to enhance the energy efficiency of the hydrogen reduction process. This includes assessing the energy required for hydrogen production and iron ore reduction, and exploring ways to minimize energy consumption.

- **Product quality:** Research focuses on improving the quality of the iron reduced by hydrogen. This includes achieving the desired chemical compositions, metallurgical properties, and purity levels of the reduced Fe.
- **Environmental Impact:** Studies assess the environmental impact of hydrogen-based reduction processes, including by-product emissions and their potential effects on air quality and greenhouse gas emissions.
- **Economic sustainability:** Researchers evaluate the economic viability of implementing hydrogen-based reduction processes in the steel industry. This includes analyzing the costs associated with hydrogen production and its impact on the overall economics of the process.

Ensuring consistent and comparable results across different experiments that use variable reducing atmospheres, such as pure H₂, mixtures with N₂, and various combinations of reducing gases like H₂, CO, and N₂, involves several meticulous strategies employed by researchers. Researchers ensure that all experiments are conducted using highly standardized setups. This includes using the same type of reactors, maintaining uniform sample sizes, and controlling the geometry and placement of samples within the reactor to ensure uniform exposure to gases. The proportions of gases in the mixtures are precisely controlled and measured using advanced gas flow and mixing systems. Gas flow rates are regulated with mass flow controllers that provide high accuracy and repeatability in the gas composition delivered to the reaction chamber. Before and after reduction, materials are characterized using techniques such as X-ray diffraction (XRD), scanning electron microscopy (SEM), and others to determine phase compositions and morphological changes. This helps ensure that the observed effects are due to the reducing atmosphere and not variations in material properties. Researchers perform multiple runs of the same experiment to check for reproducibility. This practice helps verify that the results are consistent and reliable across different experimental runs under the same conditions.

Given that there is currently no standardized methodology for hydrogen reduction worldwide and most experimental setups are based on their own original methodologies, it is very challenging to ensure consistent and comparable results across different experiments, especially regarding the influence of individual gas components on the observed reduction parameters. It has been shown that comparable results across different experiments can only be achieved when using pure hydrogen, as its higher reduction and diffusion capacity has been demonstrated in most studies. When using mixtures of reduction gases based on hydrogen (especially with an increased amount of CO), the diffusion coefficient of the reduction gas decreases, and other factors, such as the physicochemical and metallurgical properties of Fe materials and the temperature of reduction, have a major influence on the kinetics of the reduction reactions.

To understand how studies address potential confounding factors or variations in experimental conditions that might influence the observed differences in reduction rates among hydrogen (H₂), carbon monoxide (CO), or mixed gases, we can consider several key aspects of experimental design and methodology. Studies typically ensure rigorous control over experimental conditions such as temperature, pressure, and gas flow rates. These parameters are closely monitored and maintained consistently to ensure that variations in reduction rates are attributable to the gas composition rather than external variables. For example, the temperature is often precisely controlled using sophisticated furnace systems, and gas flow rates are regulated using mass flow controllers. To minimize variations due to material differences, studies often use standardized or well-characterized samples of iron oxides. This includes using pellets or powders with specified sizes, shapes, and compositions. By standardizing the materials used, researchers can more reliably attribute differences in reduction behavior to the gas composition rather than variations in the physical or chemical properties of the samples. Studies frequently include repeated trials under the same conditions to test the repeatability of the results. Additionally, experiments are often replicated under slightly varied conditions to understand how sensitive the results are to changes in experimental setups. This helps in distinguishing real effects from

experimental noise or anomalies. To specifically assess the effects of different reducing gases, experiments often involve comparative tests where everything except the type of reducing gas remains constant. This allows for a direct comparison of the effects of H₂, CO, and mixed gases on reduction rates. It is common to switch gases in the same experimental setup and measure how quickly the iron oxide reduces under each condition. By addressing these factors, research studies aim to provide a clear understanding of how different reducing gases influence the kinetics of iron oxide reduction, thereby contributing to the development of more efficient and environmentally friendly metallurgical processes. Even though there are differences in the impact of H₂, CO, and mixed gases on the reduction in iron oxides in research studies, detailed characteristics of the experiments are always provided, which help generalize the results of the reduction processes. Correlations between experiments and mathematical and thermodynamic models are also important. Therefore, the precise construction of mathematical and thermodynamic models for the direct reduction in iron oxides by H₂ and CO gases is a fundamental key to predicting the hydrodynamics, mass transfer, and heat transfer within the interaction of gases with solid matter and helps minimize potential confounding factors or variations in experimental conditions.

Researchers achieve consistent and valid findings across studies investigating the reduction potential of hydrogen (H₂), carbon monoxide (CO), and mixed gases by meticulously managing variables such as particle size, ore composition, and the specifics of the experimental setup. They regulate the size and surface area of iron ore particles across experiments to maintain uniformity, or they employ a controlled range of particle sizes to examine their influence on the reduction process. This standardization helps distinguish the effects of the gases used from the intrinsic properties of the ore. Given that the composition of different ores can vary in terms of iron oxides and gangue materials—factors that affect the reduction outcome—researchers ensure uniformity by either sourcing ores from the same batch or by conducting detailed analyses of their chemical and mineralogical properties. The configuration and operational parameters of the experimental reactors, such as fixed-bed, fluidized-bed, or rotary kilns, are also standardized to influence the interaction dynamics between gases and solids consistently. Precise regulation and monitoring of the composition and flow rate of reducing gases are crucial, typically managed with well-calibrated gas flow meters and mixing systems to guarantee that conditions are uniform across all experiments. Moreover, to understand the relationship between microstructural alterations and different reducing atmospheres, researchers utilize sophisticated analytical methods like X-ray diffraction (XRD), scanning electron microscopy (SEM), and mass spectrometry to examine the products and residues of reduction. These methods provide deep insights into how microstructural changes correlate with different reducing environments, enhancing the reliability of research conclusions.

X-ray diffraction (XRD), scanning electron microscopy (SEM), and X-ray spectroscopy (energy-dispersive spectroscopy, EDS) are critical analytical techniques used to characterize the structural and compositional changes in materials during reduction processes. Each of these techniques provides unique insights into the properties of materials, and their use is fundamental in many areas of materials science and engineering, especially when modifying the chemical and physical structures of materials. XRD helps in identifying the phase changes by detecting the arrangement and size of the crystals. The diffraction patterns obtained can show changes in peak positions, intensities, and breadths, which indicate alterations in lattice parameters, phase composition, and crystallinity. This is crucial for understanding how reduction affects the structural properties at the atomic level. SEM provides high-resolution images of the surface of materials, allowing for a detailed examination of the morphology and topography [114,115].

After a reduction process, changes in surface morphology such as particle size, agglomeration, and surface defects can be critical. SEM can visualize these changes and give insights into the surface phenomena at the micro to nanoscale. This is particularly important for evaluating how such physical changes influence the mechanical and chemical properties of materials. EDS is used alongside SEM to analyze the elemental composi-

tion of materials. It detects X-rays emitted from a sample during bombardment with an electron beam to characterize the elemental composition of the analyzed volume. During reduction, the elemental composition of a material can change significantly. EDS allows for the identification and quantification of these elements before and after the reduction. This is essential for confirming the success of the reduction process (e.g., reduction of iron oxides to elemental iron) and for determining the purity of the reduced material. These techniques are often used in tandem to provide a holistic view of material changes during processes like reduction, ensuring that all aspects of material transformation are adequately characterized [114,115].

Iron and its oxides are crystalline, meaning that the atoms are ordered in well defined repetitive crystal structures. When illuminating these materials with a beam of X-ray light, the beam will be diffracted, producing a measurable pattern of high intensity peaks. The located (angle) of these peaks is the result of constructive and destructive interference resulting from the crystal structure of the material. The produced interference pattern is therefore a “fingerprint” of the atoms present the material in combination with their orientation to each other. If a material is composed of a mixture of crystalline materials, the measured pattern is a linear combination of the individual components (multiplied by their mass fraction and inherent diffraction strength). On this principle, X-ray diffraction is based [116].

A big challenge in mineral detection, identification, and distinction using EDS spectra is that some minerals have very similar elemental compositions, such as hematite (Fe_2O_3) and magnetite (Fe_3O_4). Hematite is composed of 70% by weight Fe and 30% by weight O, while magnetite is made up of 72% by weight Fe and 28% by weight O. The EDS spectra for both minerals appear to be very similar, and the very trivial differences in Fe and O peaks cannot be resolved by appearance. In such scenarios, it is a good idea to use the BSE image gray level as an additional distinguishing standard. It must be noted that for such a measurement, a specific BSE brightness and contrast calibration is needed. Another challenge is the detection range of EDS spectra, as it does not cover the whole elemental periodic system. For example, the first light elements cannot be detected by EDS, such as H, He, Li, and Be. It is, therefore, recommended to complement EDS spectra with XRD and XRF methodologies for mineral identification and quantification. Other limitations of EDS spectra include longer mapping causing damage to the samples, low sensitivity of light elements, low quantitative accuracy, information about the chemical composition only (not about functional groups or chemical bonds), and overlapping peaks, making it difficult to distinguish among elements present in the sample. The XRD technique provides insights about crystalline structures; however, it does not reveal any valuable information about amorphous materials—a limitation. XRD works quite well with single-phase and homogenous minerals; however, it does not demonstrate accuracy with mixed materials, with which the detection limit of XRD is about 4 wt.% of the sample. Now we have the possibility to attach cooling and heating stages, and it is possible to make measurements with variations in temperature profiles and their effect on crystal parameters [117].

In the synthesis of findings presented in this article, a methodological approach was employed, primarily focusing on studies that utilized comparable materials under similar experimental conditions—such as temperatures and compositions of reducing gases. The conclusions drawn herein are derived from analyses and outcomes observed in studies where hydrogen was employed as the reducing agent. This approach ensures a systematic comparison, enhancing the reliability and validity of the synthesized conclusions by aligning experimental variables across different research contexts.

The laboratory experiments discussed in this article primarily focused on the reduction of ores, pellets, and synthetic powders. The size of the samples and their grain sizes largely depended on the dimensions of the experimental equipment used. The methods employed for reducing various materials with hydrogen varied significantly. There is no standardized or universally accepted method for hydrogen reduction at the global level. Most of the experimental apparatus used in these studies were custom-built based on original

methodologies, and their creators adapted these setups according to the characteristics of the specific samples and the reduction parameters they were monitoring. Commonly used methods included those based on TGA (Thermogravimetric Analysis) devices, fluidized beds, and reduction retorts.

Most studies have focused on determining the reduction potential of H₂. Researchers agree that the reduction process using H₂ occurs more intensively and quickly than with pure CO or an H₂/CO mixture.

Temperature is one of the most crucial factors influencing the hydrogen reduction process. Reduction is more intense at higher temperatures, typically around 800 °C, which significantly enhances both the reaction rate and the degree of reduction. Increasing the temperature leads to an increase in these parameters. Conversely, some iron ore grains can be effectively reduced even at lower temperatures, approximately 600 °C.

Overall, the reduction of Fe₂O₃ to Fe₃O₄ and Fe₃O₄ to FeO occurs very quickly. The slowest step in the reduction reactions is the transformation of FeO into metallic Fe. In the initial stages of reduction, the reduction rate is high and the degree of reduction increases rapidly. However, in the later stages, this increase becomes less pronounced due to the resistance offered by the product layer. An increase in H₂ flow positively affects the degree of reduction; higher flow rates lead to greater reduction. Several studies have addressed the influence of the composition of the reduced material. The reduction in hematite by hydrogen is generally faster than that of magnetite, especially at higher temperatures. These studies have shown that the degree of reduction is primarily affected by factors such as porosity—whether initial or developed due to phase changes and temperature—and the surface area. Regarding particle size, it has been found that for particles smaller than 0.045 mm, the reduction rate is not significantly influenced because, at these sizes, internal diffusion resistance is negligible. However, for larger particles, size does impact reduction rates, mainly through diffusivity. In terms of pressure, research has indicated a subtle impact of the absolute pressure of the gas mixture, within a range of 1 to 3 bars, on the kinetics of the reduction process. Conversely, an increase in the partial pressure of reducing gases notably enhances the reduction kinetics. The main conclusions from the literature review are illustrated in the diagram in Figure 15.

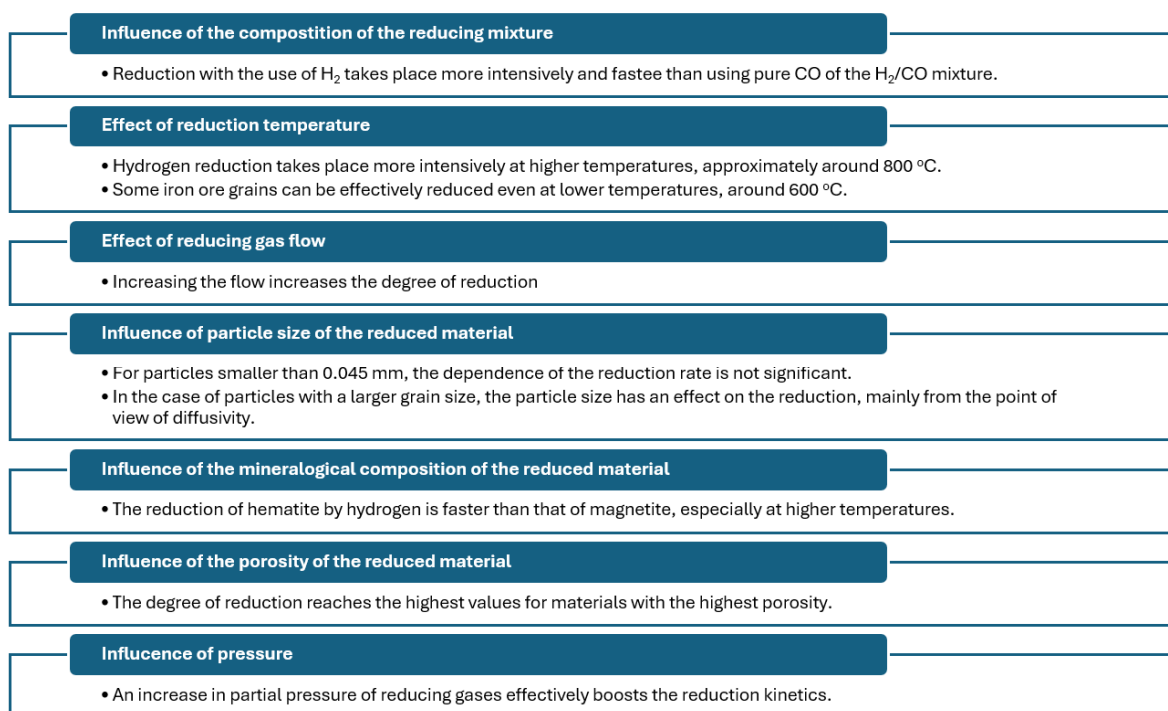


Figure 15. Scheme of the most significant conclusions from the literature research.

In their publications, the authors extensively discussed the impact of physical properties, such as porosity and pellet diameter, on the rate of hydrogen reduction. Generally, the rate of reduction decreases as the pellet diameter increases. Concurrently, it has been observed that the reduction is most effective in pellets with the highest porosity. Iron-based pellets undergo volume changes influenced by the reducing atmosphere and the temperature at which reduction occurs. Additionally, the studies revisited the effect of adding biomass to the pellets and concluded that this inclusion positively affects the porosity of the resulting pellets.

4. Conclusions

Research into the use of hydrogen in metallurgy, particularly during reduction processes, is currently a topic of considerable interest. Laboratory research should be oriented towards achieving practical results that could underpin further technology development and implementation in industrial applications. This research should also aid in developing innovative and sustainable iron production methods that do not produce high levels of CO₂ emissions. Researchers are focused on optimizing reduction conditions and developing new methodologies and technologies aimed at streamlining and enhancing hydrogen reduction processes in metallurgy. In this way, it is possible to achieve not only economic benefits, but also environmental sustainability in metallurgical reduction processes. As part of this effort, an analysis and study of the current knowledge was conducted, with an emphasis on the applications of hydrogen as a reducing agent in the metallurgical processes of iron and steel production. The analysis indicates that hydrogen, as an environmentally friendly reducing agent, holds significant potential for use in reducing Fe commodities. Currently, however, there are several limitations and challenges that hinder its broader use, such as the cost of hydrogen production, safety issues, and the need for changes in infrastructure and existing technologies. Addressing these challenges could bring the use of hydrogen as a reducing agent in metallurgy closer to practical application and help achieve ecological goals in the metal mining and processing industry.

Author Contributions: Conceptualization, Z.M.; methodology, Z.M.; validation, J.L.; formal analysis, Z.M.; investigation, Z.M.; resources, Z.M., J.L., P.D., B.B., S.H., M.H., P.F. and R.F.; data curation, Z.M.; writing—original draft preparation, Z.M.; writing—review and editing, J.L., P.D., B.B., S.H., M.H., P.F. and R.F.; visualization, Z.M.; supervision, J.L. and Z.M.; project administration, J.L. and Z.M.; funding acquisition, J.L. All authors have read and agreed to the published version of the manuscript.

Funding: This research was funded by the Slovak Research and Development Agency (APVV), Slovak Republic, No. APVV-21-0142.

Data Availability Statement: The raw data supporting the conclusions of this article will be made available by the authors on request.

Conflicts of Interest: The authors declare no conflicts of interest.

References

1. Wang, R.R.; Zhao, Y.Q.; Babich, A.; Senk, D.; Fan, X.Y. Hydrogen Direct Reduction (H-DR) in Steel Industry—An Overview of Challenges and Opportunities. *J. Clean. Prod.* **2021**, *329*, 129797. [\[CrossRef\]](#)
2. Okolie, J.A.; Patra, B.R.; Mukherjee, A.; Nanda, S.; Dalai, A.K.; Kozinski, J.A. Futuristic Applications of Hydrogen in Energy, Biorefining, Aerospace, Pharmaceuticals and Metallurgy. *Int. J. Hydrogen Energy* **2021**, *46*, 8885–8905. [\[CrossRef\]](#)
3. Hasanbeigi, A.; Arens, M.; Cardenas, J.C.R.; Price, L.; Triolo, R. Comparison of Carbon Dioxide Emissions Intensity of Steel Production in China, Germany, Mexico, and the United States. *Resour. Conserv. Recycl.* **2016**, *113*, 127–139. [\[CrossRef\]](#)
4. Vogl, V.; Åhman, M.; Nilsson, L.J. Assessment of Hydrogen Direct Reduction for Fossil-Free Steelmaking. *J. Clean. Prod.* **2018**, *203*, 736–745. [\[CrossRef\]](#)
5. Morfeldt, J.; Nijs, W.; Silveira, S. The Impact of Climate Targets on Future Steel Production—An Analysis Based on a Global Energy System Model. *J. Clean. Prod.* **2015**, *103*, 469–482. [\[CrossRef\]](#)
6. Ariyama, T.; Takahashi, K.; Kawashiri, Y.; Nouchi, T. Diversification of the Ironmaking Process toward the Long-Term Global Goal for Carbon Dioxide Mitigation. *J. Sustain. Metall.* **2019**, *5*, 276–294. [\[CrossRef\]](#)

7. Bataille, C.; Åhman, M.; Neuhoff, K.; Nilsson, L.J.; Fishedick, M.; Lechtenböhmer, S.; Solano-Rodriguez, B.; Denis-Ryan, A.; Stiebert, S.; Waisman, H.; et al. A Review of Technology and Policy Deep Decarbonization Pathway Options for Making Energy-Intensive Industry Production Consistent with the Paris Agreement. *J. Clean. Prod.* **2018**, *187*, 960–973. [CrossRef]
8. Li, Z.; Davis, C. Ironmaking and Steelmaking. *Metals* **2019**, *9*, 525. [CrossRef]
9. Nikolaidis, P.; Poullikkas, A. A Comparative Overview of Hydrogen Production Processes. *Renew. Sustain. Energy Rev.* **2017**, *67*, 597–611. [CrossRef]
10. Ma, K.; Deng, J.; Wang, G.; Zhou, Q.; Xu, J. Utilization and Impacts of Hydrogen in the Ironmaking Processes: A Review from Lab-Scale Basics to Industrial Practices. *Int. J. Hydrogen Energy* **2021**, *46*, 26646–26664. [CrossRef]
11. Mazloomi, K.; Gomes, C. Hydrogen as an Energy Carrier: Prospects and Challenges. *Renew. Sustain. Energy Rev.* **2012**, *16*, 3024–3033. [CrossRef]
12. Wietschel, M.; Hasenauer, U.; de Groot, A. Development of European Hydrogen Infrastructure Scenarios—CO₂ Reduction Potential and Infrastructure Investment. *Energy Policy* **2006**, *34*, 1284–1298. [CrossRef]
13. Sun, M.; Pang, K.; Barati, M.; Meng, X. Hydrogen-Based Reduction Technologies in Low-Carbon Sustainable Ironmaking and Steelmaking: A Review. *J. Sustain. Metall.* **2024**, *10*, 10–25. [CrossRef]
14. Fan, Z.; Friedmann, S.J. Low-Carbon Production of Iron and Steel: Technology Options, Economic Assessment, and Policy. *Joule* **2021**, *5*, 829–862. [CrossRef]
15. Liu, W.; Zuo, H.; Wang, J.; Xue, Q.; Ren, B.; Yang, F. The Production and Application of Hydrogen in Steel Industry. *Int. J. Hydrogen Energy* **2021**, *46*, 10548–10569. [CrossRef]
16. Chen, Y.; Zuo, H. Review of Hydrogen-Rich Ironmaking Technology in Blast Furnace. *Ironmak. Steelmak.* **2021**, *48*, 749–768. [CrossRef]
17. Yilmaz, C.; Wendelstorf, J.; Turek, T. Modeling and Simulation of Hydrogen Injection into a Blast Furnace to Reduce Carbon Dioxide Emissions. *J. Clean. Prod.* **2017**, *154*, 488–501. [CrossRef]
18. Mittemeijer, E.J. Steel Heat Treating Fundamentals and Processes. In *ASM Handbook*; Dossett, J., Totten, G.E., Eds.; Introduction to Surface Hardening of Steels; ASM International: Detroit, MI, USA, 2013; Volume 4A, p. 784.
19. Quader, M.A.; Ahmed, S.; Ghazilla, R.A.R.; Ahmed, S.; Dahari, M. A Comprehensive Review on Energy Efficient CO₂ Break-through Technologies for Sustainable Green Iron and Steel Manufacturing. *Renew. Sustain. Energy Rev.* **2015**, *50*, 594–614. [CrossRef]
20. Cavaliere, P. Direct Reduced Iron: Most Efficient Technologies for Greenhouse Emissions Abatement. In *Clean Ironmaking and Steelmaking Processes*; Springer: Cham, Switzerland, 2019; pp. 419–484. [CrossRef]
21. Jiang, X.; Wang, L.; Shen, F.M. Shaft Furnace Direct Reduction Technology—Midrex and Energiron. *Adv. Mat. Res.* **2013**, *805–806*, 654–659. [CrossRef]
22. Tang, J.; Chu, M.S.; Li, F.; Feng, C.; Liu, Z.G.; Zhou, Y.S. Development and Progress on Hydrogen Metallurgy. *Int. J. Miner. Metall. Mater.* **2020**, *27*, 713–723. [CrossRef]
23. Zhang, X.; Jiao, K.; Zhang, J.; Guo, Z. A Review on Low Carbon Emissions Projects of Steel Industry in the World. *J. Clean. Prod.* **2021**, *306*, 127259. [CrossRef]
24. Pei, M.; Petäjäniemi, M.; Regnell, A.; Wijk, O. Toward a Fossil Free Future with HYBRIT: Development of Iron and Steelmaking Technology in Sweden and Finland. *Metals* **2020**, *10*, 972. [CrossRef]
25. The Adoption of Hydrogen Metallurgy in the Climate-Neutral Production of Steel | HELIOS | Project | Fact Sheet | HORIZON | CORDIS | European Commission. Available online: <https://cordis.europa.eu/project/id/101120068> (accessed on 25 November 2023).
26. Green H₂ and Circular Bio-Coal from Biowaste for Cost-Competitive Sustainable Steel | H₂STEEL | Project | Fact Sheet | HORIZON | CORDIS | European Commission. Available online: <https://cordis.europa.eu/project/id/101070741> (accessed on 25 November 2023).
27. Hydrogen Technologies for Decarbonization of Industrial Heating Processes | HyInHeat | Project | Fact Sheet | HORIZON | CORDIS | European Commission. Available online: <https://cordis.europa.eu/project/id/101091456> (accessed on 25 November 2023).
28. Hybrid Hydrogen-Based Reduction of Iron Ores | Max-Planck-Institut Für Eisenforschung GmbH. Available online: https://www.mpie.de/4728546/hybrid_hydrogen-based_reduction (accessed on 25 November 2023).
29. Hydrogen Plasma-Based Reduction of Iron Ores | Max-Planck-Institut Für Eisenforschung GmbH. Available online: https://www.mpie.de/4727993/hydrogen_plasma-based_reduction (accessed on 25 November 2023).
30. Hydrogen As the Reducing Agent in the REcovery of Metals and Minerals from Metallurgical Waste | HARARE | Project | Fact Sheet | H₂2020 | CORDIS | European Commission. Available online: <https://cordis.europa.eu/project/id/958307> (accessed on 28 January 2024).
31. Decarbonising Steel Production in China: H₂-DRI-EAF Technology. Available online: https://transitionasia.org/wp-content/uploads/2024/02/TA_DecarbonisingSteelProductionInChina_Feb2024N.pdf (accessed on 14 May 2024).
32. Öhman, A.; Karakaya, E.; Urban, F. Enabling the Transition to a Fossil-Free Steel Sector: The Conditions for Technology Transfer for Hydrogen-Based Steelmaking in Europe. *Energy Res. Soc. Sci.* **2022**, *84*, 102384. [CrossRef]
33. Oh, J.; Noh, D. The Reduction Kinetics of Hematite Particles in H₂ and CO Atmospheres. *Fuel* **2017**, *196*, 144–153. [CrossRef]
34. Hessling, O.; Tottie, M.; Sichen, D. Experimental Study on Hydrogen Reduction of Industrial Fines in Fluidized Bed. *Ironmak. Steelmak.* **2021**, *48*, 936–943. [CrossRef]

35. Bai, M.; Long, H.; Li, L.; Liu, D.; Ren, S.B.; Zhao, C.F.; Cheng, J. Kinetics of Iron Ore Pellets Reduced by H₂-N₂ under Non-Isothermal Condition. *Int. J. Hydrogen Energy* **2018**, *43*, 15586–15592. [[CrossRef](#)]
36. Wei, Z.; Zhang, J.; Qin, B.; Dong, Y.; Lu, Y.; Li, Y.; Hao, W.; Zhang, Y. Reduction Kinetics of Hematite Ore Fines with H₂ in a Rotary Drum Reactor. *Powder Technol.* **2018**, *332*, 18–26. [[CrossRef](#)]
37. Nyankson, E.; Kolbeinsen, L. Kinetics of Direct Iron Ore Reduction with CO-H₂ Gas Mixtures. *Int. J. Eng. Res. Technol.* **2015**, *4*, 934–940. [[CrossRef](#)]
38. Chen, Z.; Dang, J.; Hu, X.; Yan, H. Reduction Kinetics of Hematite Powder in Hydrogen Atmosphere at Moderate Temperatures. *Metals* **2018**, *8*, 751. [[CrossRef](#)]
39. Spreitzer, D.; Schenk, J. Iron Ore Reduction by Hydrogen Using a Laboratory Scale Fluidized Bed Reactor: Kinetic Investigation-Experimental Setup and Method for Determination. *Metall. Mater. Trans. B* **2019**, *50*, 2471–2484. [[CrossRef](#)]
40. Wang, D.; Sichen, D. Effect of Density on the Reduction of Fe₂O₃ Pellets by H₂-CO Mixtures. Master's Thesis, School of Industrial Engineering and Management, Royal Institute of Technology, Stockholm, Sweden, 2023.
41. Zhang, J.; Li, Y.; Liu, Z.; Wang, T.; Wang, Y.; Li, K.; Wang, G.; Xu, T.; Zhang, Y. Isothermal Kinetic Analysis on Reduction of Solid/Liquid Wustite by Hydrogen. *Int. J. Miner. Metall. Mater.* **2022**, *29*, 1830–1838. [[CrossRef](#)]
42. Du, W.; Yang, S.; Pan, F.; Shangguan, J.; Lu, J.; Liu, S.; Fan, H. Hydrogen Reduction of Hematite Ore Fines to Magnetite Ore Fines at Low Temperatures. *J. Chem.* **2017**, *2017*, 1919720. [[CrossRef](#)]
43. Wagner, D.; Devisme, O.; Patisson, F.; Ablitzer, D. A Laboratory Study of The Reduction of Iron Oxides by Hydrogen. In Proceedings of the Sohn International Symposium, San Diego, CA, USA, 27–31 August 2006.
44. Kuila, S.K.; Chatterjee, R.; Ghosh, D. Kinetics of Hydrogen Reduction of Magnetite Ore Fines. *Int. J. Hydrogen Energy* **2016**, *41*, 9256–9266. [[CrossRef](#)]
45. Spreitzer, D.; Schenk, J. Fluidization Behavior and Reducibility of Iron Ore Fines during Hydrogen-Induced Fluidized Bed Reduction. *Particuology* **2020**, *52*, 36–46. [[CrossRef](#)]
46. Qu, Y.; Xing, L.; Shao, L.; Luo, Y.; Zou, Z. Microstructural Characterization and Gas-Solid Reduction Kinetics of Iron Ore Fines at High Temperature. *Powder Technol.* **2019**, *355*, 26–36. [[CrossRef](#)]
47. Zhang, T.; Lei, C.; Zhu, Q. Reduction of Fine Iron Ore via a Two-Step Fluidized Bed Direct Reduction Process. *Powder Technol.* **2014**, *254*, 1–11. [[CrossRef](#)]
48. Guo, D.; Hu, M.; Pu, C.; Xiao, B.; Hu, Z.; Liu, S.; Wang, X.; Zhu, X. Kinetics and Mechanisms of Direct Reduction of Iron Ore-Biomass Composite Pellets with Hydrogen Gas. *Int. J. Hydrogen Energy* **2015**, *40*, 4733–4740. [[CrossRef](#)]
49. Kazemi, M.; Pour, M.S.; Sichen, D. Experimental and Modeling Study on Reduction of Hematite Pellets by Hydrogen Gas. *Metall. Mater. Trans. B Process Metall. Mater. Process. Sci.* **2017**, *48*, 1114–1122. [[CrossRef](#)]
50. Jozwiak, W.K.; Kaczmarek, E.; Maniecki, T.P.; Ignaczak, W.; Maniukiewicz, W. Reduction Behavior of Iron Oxides in Hydrogen and Carbon Monoxide Atmospheres. *Appl. Catal. A Gen.* **2007**, *326*, 17–27. [[CrossRef](#)]
51. Zuo, H.B.; Wang, C.; Dong, J.J.; Jiao, K.X.; Xu, R.S. Reduction Kinetics of Iron Oxide Pellets with H₂ and CO Mixtures. *Int. J. Miner. Metall. Mater.* **2015**, *22*, 688–696. [[CrossRef](#)]
52. Kim, W.H.; Lee, S.; Kim, S.M.; Min, D.J. The Retardation Kinetics of Magnetite Reduction Using H₂ and H₂-H₂O Mixtures. *Int. J. Hydrogen Energy* **2013**, *38*, 4194–4200. [[CrossRef](#)]
53. Ngoy, D.; Sukhomlinov, D.; Tangstad, M. Pre-Reduction Behaviour of Manganese Ores in H₂ and CO Containing Gases. *ISIJ Int.* **2020**, *60*, 2325–2331. [[CrossRef](#)]
54. Li, P.; Li, Y.; Yu, J.; Gao, P.; Han, Y. Kinetics and Microstructural Changes during Fluidized Reduction of Magnetite with Hydrogen at Low Temperatures. *Int. J. Hydrogen Energy* **2022**, *47*, 31140–31151. [[CrossRef](#)]
55. Li, S.; Zhang, H.; Nie, J.; Dewil, R.; Baeyens, J.; Deng, Y. The Direct Reduction of Iron Ore with Hydrogen. *Sustainability* **2021**, *13*, 8866. [[CrossRef](#)]
56. Zheng, H.; Daghighaleh, O.; Wolfinger, T.; Taferner, B.; Schenk, J.; Xu, R. Fluidization Behavior and Reduction Kinetics of Pre-Oxidized Magnetite-Based Iron Ore in a Hydrogen-Induced Fluidized Bed. *Int. J. Miner. Metall. Mater.* **2022**, *29*, 1873–1881. [[CrossRef](#)]
57. Dhawan, N.; Manzoor, U.; Agrawal, S.; Dhawan, N.; Manzoor, U.; Agrawal, S. Hydrogen Reduction of Low-Grade Banded Iron Ore. *MiEng* **2022**, *187*, 107794. [[CrossRef](#)]
58. Scharm, C.; Küster, F.; Laabs, M.; Huang, Q.; Volkova, O.; Reinmöller, M.; Guhl, S.; Meyer, B. Direct Reduction of Iron Ore Pellets by H₂ and CO: In-Situ Investigation of the Structural Transformation and Reduction Progression Caused by Atmosphere and Temperature. *Miner. Eng.* **2022**, *180*, 107459. [[CrossRef](#)]
59. Lyu, Q.; Qie, Y.; Liu, X.; Lan, C.; Li, J.; Liu, S. Effect of Hydrogen Addition on Reduction Behavior of Iron Oxides in Gas-Injection Blast Furnace. *Thermochim. Acta* **2017**, *648*, 79–90. [[CrossRef](#)]
60. Abu Tahari, M.N.; Salleh, F.; Tengku Saharuddin, T.S.; Samsuri, A.; Samidin, S.; Yarmo, M.A. Influence of Hydrogen and Carbon Monoxide on Reduction Behavior of Iron Oxide at High Temperature: Effect on Reduction Gas Concentrations. *Int. J. Hydrogen Energy* **2021**, *46*, 24791–24805. [[CrossRef](#)]
61. Hessels, C.J.M.; Homan, T.A.M.; Deen, N.G.; Tang, Y. Reduction Kinetics of Combusted Iron Powder Using Hydrogen. *Powder Technol.* **2022**, *407*, 117540. [[CrossRef](#)]
62. El-Geassy, A.A.; Nasr, M.I. Influence of the Original Structure on the Kinetics of Hydrogen Reduction of Hematite Compacts. *Trans. Iron Steel Inst. Jpn.* **1988**, *28*, 650–658. [[CrossRef](#)]

63. He, J.; Li, K.; Zhang, J.; Conejo, A.N. Reduction Kinetics of Compact Hematite with Hydrogen from 600 to 1050 °C. *Metals* **2023**, *13*, 464. [[CrossRef](#)]
64. Bahgat, M.; Khedr, M.H. Reduction Kinetics, Magnetic Behavior and Morphological Changes during Reduction of Magnetite Single Crystal. *Mater. Sci. Eng. B* **2007**, *138*, 251–258. [[CrossRef](#)]
65. Zieliński, J.; Zglinicka, I.; Znak, L.; Kaszkur, Z. Reduction of Fe₂O₃ with Hydrogen. *Appl. Catal. A Gen.* **2010**, *381*, 191–196. [[CrossRef](#)]
66. Barde, A.A.; Klausner, J.F.; Mei, R. Solid State Reaction Kinetics of Iron Oxide Reduction Using Hydrogen as a Reducing Agent. *Int. J. Hydrogen Energy* **2016**, *41*, 10103–10119. [[CrossRef](#)]
67. Heidari, A.; Niknahad, N.; Iljana, M.; Fabritius, T. A Review on the Kinetics of Iron Ore Reduction by Hydrogen. *Materials* **2021**, *14*, 7540. [[CrossRef](#)] [[PubMed](#)]
68. Hidayat, T.; Shishin, D.; Jak, E.; Decterov, S.A. Thermodynamic Reevaluation of the Fe–O System. *Calphad* **2015**, *48*, 131–144. [[CrossRef](#)]
69. Kawasaki, E.; Sanscrainte, J.; Walsh, T.J. Kinetics of Reduction of Iron Oxide with Carbon Monoxide and Hydrogen. *AIChE J.* **1962**, *8*, 48–52. [[CrossRef](#)]
70. Ma, Y.; Souza Filho, I.R.; Bai, Y.; Schenk, J.; Patisson, F.; Beck, A.; van Bokhoven, J.A.; Willinger, M.G.; Li, K.; Xie, D.; et al. Hierarchical Nature of Hydrogen-Based Direct Reduction of Iron Oxides. *Scr. Mater.* **2022**, *213*, 114571. [[CrossRef](#)]
71. Bhaskar, A.; Assadi, M.; Somehsaraei, H.N. Decarbonization of the Iron and Steel Industry with Direct Reduction of Iron Ore with Green Hydrogen. *Energies* **2020**, *13*, 758. [[CrossRef](#)]
72. Hammam, A.; Nasr, M.I.; Elsadek, M.H.; Khan, I.U.; Omran, M.; Wei, H.; Qiu, D.; Yu, Y. Studies on the Reduction Behavior of Iron Oxide Pellet Fines with Hydrogen Gas: Mechanism and Kinetic Analysis. *J. Sustain. Metall.* **2023**, *9*, 1289–1302. [[CrossRef](#)]
73. He, K.; Zheng, Z.; Chen, Z.; Chen, H.; Hao, W. Kinetics of Hydrogen Reduction of Brazilian Hematite in a Micro-Fluidized Bed. *Int. J. Hydrogen Energy* **2021**, *46*, 4592–4605. [[CrossRef](#)]
74. Mao, X.; Garg, P.; Hu, X.; Li, Y.; Nag, S.; Kundu, S.; Zhang, J. Kinetic Analysis of Iron Ore Powder Reaction with Hydrogen—Carbon Monoxide. *Int. J. Miner. Metall. Mater.* **2022**, *29*, 1882–1890. [[CrossRef](#)]
75. Fogelström, J.B.; Martinsson, J.; Kojola, N. The Influence of Nitrogen on Hydrogen Reduction of Iron Ore Pellets. *Steel Res. Int.* **2024**, *95*, 2300655. [[CrossRef](#)]
76. Lyu, B.; Wang, G.; Yang, F.; Zuo, H.; Xue, Q.; Wang, J. Kinetic Analysis of Isothermal and Non-Isothermal Reduction of Iron Ore Fines in Hydrogen Atmosphere. *Metals* **2022**, *12*, 1754. [[CrossRef](#)]
77. Teplov, O.A. Kinetics of the Low-Temperature Hydrogen Reduction of Magnetite Concentrates. *Russ. Metall. Met.* **2012**, *2012*, 8–21. [[CrossRef](#)]
78. Abdelrahim, A.; Iljana, M.; Omran, M.; Vuolio, T.; Bartusch, H.; Fabritius, T. Influence of H₂–H₂O Content on the Reduction of Acid Iron Ore Pellets in a CO–CO₂–N₂ Reducing Atmosphere. *ISIJ Int.* **2020**, *60*, 2206–2217. [[CrossRef](#)]
79. He, K.; Zheng, Z.; Chen, H.; Hao, W. Reduction Behaviors of Hematite to Metallic Iron by Hydrogen at Low Temperatures. In *Minerals, Metals and Materials Series*; Springer: Cham, Switzerland, 2021; pp. 111–122. [[CrossRef](#)]
80. Yi, L.; Huang, Z.; Peng, H.; Jiang, T. Action Rules of H₂ and CO in Gas-Based Direct Reduction of Iron Ore Pellets. *J. Cent. South Univ.* **2012**, *19*, 2291–2296. [[CrossRef](#)]
81. Kang, H.; Xu, Q.; Cao, Z.; Lu, X.; Shi, J.; Chen, B.; Guo, L. Influence of Hydrogen Flow Rate on Multistep Kinetics of Hematite Reduction. *Int. J. Hydrogen Energy* **2024**, *49*, 1255–1268. [[CrossRef](#)]
82. Mirzajani, A.; Ale Ebrahim, H.; Nouri, S.M.M. Simulation of a Direct Reduction Moving Bed Reactor Using a Three Interface Model. *Braz. J. Chem. Eng.* **2018**, *35*, 1019–1028. [[CrossRef](#)]
83. Wolfinger, T.; Spreitzer, D.; Schenk, J. Using Iron Ore Ultra-Fines for Hydrogen-Based Fluidized Bed Direct Reduction—A Mathematical Evaluation. *Materials* **2022**, *15*, 3943. [[CrossRef](#)] [[PubMed](#)]
84. Olivares, B.; René, I. Reduction of Iron Ore in a Batch Fluidized Bed. Master’s Thesis, University of New South Wales, Sydney, Australia, 1990. [[CrossRef](#)]
85. Heikkilä, A.; Iljana, M.; Bartusch, H.; Fabritius, T. Reduction of Iron Ore Pellets, Sinter, and Lump Ore under Simulated Blast Furnace Conditions. *Steel Res. Int.* **2020**, *91*, 2000047. [[CrossRef](#)]
86. Hou, B.; Zhang, H.; Li, H.; Zhu, Q. Study on Kinetics of Iron Oxide Reduction by Hydrogen. *Chin. J. Chem. Eng.* **2012**, *20*, 10–17. [[CrossRef](#)]
87. Sundberg, R. Reduction of Iron Oxides with Hydrogen. Master’s Thesis, Abo Akademi University, Turku, Finland, 2021.
88. Souza Filho, I.R.; Ma, Y.; Raabe, D.; Springer, H. Fundamentals of Green Steel Production: On the Role of Gas Pressure During Hydrogen Reduction of Iron Ores. *JOM* **2023**, *75*, 2274–2286. [[CrossRef](#)] [[PubMed](#)]
89. Sato, K.; Ueda, Y.; Nishikawa, Y.; Goto, T. Effect of Pressure on Reduction Rate of Iron Ore with High Pressure Fluidized Bed. *Trans. Iron Steel Inst. Jpn.* **1986**, *26*, 697–703. [[CrossRef](#)]
90. Habermann, A.; Winter, F.; Hofbauer, H.; Zirngast, J.; Schenk, J.L. An Experimental Study on the Kinetics of Fluidized Bed Iron Ore Reduction. *ISIJ Int.* **2000**, *40*, 935–942. [[CrossRef](#)]
91. Sato, K.; Nishikawa, Y.; Tamura, I. Pressure Increase and Temperature Fall within a Hematite Sphere during Reduction by Hydrogen. *Tetsu–Hagane* **1983**, *69*, 1137–1144. [[CrossRef](#)] [[PubMed](#)]
92. Spreitzer, D.; Schenk, J. Reduction of Iron Oxides with Hydrogen—A Review. *Steel Res. Int.* **2019**, *90*, 1900108. [[CrossRef](#)]

93. Zare Ghadi, A.; Valipour, M.S.; Vahedi, S.M.; Sohn, H.Y. A Review on the Modeling of Gaseous Reduction of Iron Oxide Pellets. *Steel Res. Int.* **2020**, *91*, 1900270. [[CrossRef](#)]
94. Biswas, A.K. *Principles of Blast Furnace Ironmaking: Theory and Practice*; Cootha: Cootha, Australia, 1981; ISBN 0949917087/9780949917089.
95. Geerdes, M.; Chaigneau, R.; Kurunov, I.; Lingiardi, O.; Ricketts, J. *Modern Blast Furnace Ironmaking: An Introduction*, 3rd ed.; Delft University Press: Delft, The Netherlands, 2015; ISBN 978-1-61499-498-5 (Print), 978-1-61499-499-2 (Online).
96. Cavaliere, P.; Dijon, L.; Laska, A.; Koszelow, D. Hydrogen Direct Reduction and Reoxidation Behaviour of High-Grade Pellets. *Int. J. Hydrogen Energy* **2024**, *49*, 1235–1254. [[CrossRef](#)]
97. Cavaliere, P.; Perrone, A.; Dijon, L.; Laska, A.; Koszelow, D. Direct Reduction of Pellets through Hydrogen: Experimental and Model Behaviour. *Int. J. Hydrogen Energy* **2024**, *49*, 1444–1460. [[CrossRef](#)]
98. Korobeinikov, Y.; Meshram, A.; Harris, C.; Kovtun, O.; Govro, J.; O'Malley, R.J.; Volkova, O.; Sridhar, S. Reduction of Iron-Ore Pellets Using Different Gas Mixtures and Temperatures. *Steel Res. Int.* **2023**, *94*, 2300066. [[CrossRef](#)]
99. Zhang, A.; Monaghan, B.J.; Longbottom, R.J.; Nusseh, M.; Bumby, C.W. Reduction Kinetics of Oxidized New Zealand Ironsand Pellets in H₂ at Temperatures up to 1443 K. *Metall. Mater. Trans. B Process Metall. Mater. Process. Sci.* **2020**, *51*, 492–504. [[CrossRef](#)]
100. Metolina, P.; Ribeiro, T.R.; Guardani, R. Hydrogen-Based Direct Reduction of Industrial Iron Ore Pellets: Statistically Designed Experiments and Computational Simulation. *Int. J. Miner. Metall. Mater.* **2022**, *29*, 1908–1921. [[CrossRef](#)]
101. Ma, Y.; Souza Filho, I.R.; Zhang, X.; Nandy, S.; Barriobero-Vila, P.; Requena, G.; Vogel, D.; Rohwerder, M.; Ponge, D.; Springer, H.; et al. Hydrogen-Based Direct Reduction of Iron Oxide at 700 °C: Heterogeneity at Pellet and Microstructure Scales. *Int. J. Miner. Metall. Mater.* **2022**, *29*, 1901–1907. [[CrossRef](#)]
102. Bai, M.H.; Long, H.; Ren, S.B.; Liu, D.; Zhao, C.F. Reduction Behavior and Kinetics of Iron Ore Pellets under H₂-N₂ Atmosphere. *ISIJ Int.* **2018**, *58*, 1034–1041. [[CrossRef](#)]
103. Kovtun, O.; Levchenko, M.; Ilatovskaia, M.O.; Aneziris, C.G.; Volkova, O. Results of Hydrogen Reduction of Iron Ore Pellets at Different Temperatures. *Steel Res. Int.* **2024**, *10–11*, 2300707. [[CrossRef](#)]
104. Patisson, F.; Mirgaux, O. Hydrogen Ironmaking: How It Works. *Metals* **2020**, *10*, 922. [[CrossRef](#)]
105. Zhao, Z.; Tang, J.; Chu, M.; Wang, X.; Zheng, A.; Wang, X.; Li, Y. Direct Reduction Swelling Behavior of Pellets in Hydrogen-Based Shaft Furnaces under Typical Atmospheres. *Int. J. Miner. Metall. Mater.* **2022**, *29*, 1891–1900. [[CrossRef](#)]
106. Kovtun, O.; Levchenko, M.; Oldinski, E.; Gräbner, M.; Volkova, O. Swelling Behavior of Iron Ore Pellets during Reduction in H₂ and N₂/H₂ Atmospheres at Different Temperatures. *Steel Res. Int.* **2023**, *94*, 2300140. [[CrossRef](#)]
107. Yi, L.; Huang, Z.; Jiang, T.; Wang, L.; Qi, T. Swelling Behavior of Iron Ore Pellet Reduced by H₂-CO Mixtures. *Powder Technol.* **2015**, *269*, 290–295. [[CrossRef](#)]
108. Sharma, T.; Gupta, R.C.; Prakash, B. Effect of Gangue Content on the Swelling Behaviour of Iron Ore Pellets. *Miner. Eng.* **1990**, *3*, 509–516. [[CrossRef](#)]
109. Behera, P.R.; Bhoi, B.; Paramguru, R.K.; Mukherjee, P.S.; Mishra, B.K. Hydrogen Plasma Smelting Reduction of Fe₂O₃. *Metall. Mater. Trans. B Process Metall. Mater. Process. Sci.* **2019**, *50*, 262–270. [[CrossRef](#)]
110. Sabat, K.C.; Murphy, A.B. Hydrogen Plasma Processing of Iron Ore. *Metall. Mater. Trans. B Process Metall. Mater. Process. Sci.* **2017**, *48*, 1561–1594. [[CrossRef](#)]
111. Souza Filho, I.R.; Springer, H.; Ma, Y.; Mahajan, A.; da Silva, C.C.; Kulse, M.; Raabe, D. Green Steel at Its Crossroads: Hybrid Hydrogen-Based Reduction of Iron Ores. *J. Clean. Prod.* **2022**, *340*, 130805. [[CrossRef](#)]
112. Shahabuddin, M.; Brooks, G.; Rhamdhani, M.A. Decarbonisation and Hydrogen Integration of Steel Industries: Recent Development, Challenges and Technoeconomic Analysis. *J. Clean. Prod.* **2023**, *395*, 136391. [[CrossRef](#)]
113. Boretti, A. The Perspective of Hydrogen Direct Reduction of Iron. *J. Clean. Prod.* **2023**, *429*, 139585. [[CrossRef](#)]
114. Cullity, B.D.; Stock, S.R. *Elements of X-ray Diffraction*, 3rd ed.; Pearson Education Limited: Harlow, UK, 2015; ISBN 978-1-292-04054-7.
115. Goldstein, J.I.; Newbury, D.E.; Michael, J.R.; Ritchie, N.W.M.; Scott, J.H.J.; Joy, D.C. *Scanning Electron Microscopy and X-ray Microanalysis*; Springer: New York, NY, USA, 2017; 550p. [[CrossRef](#)]
116. Hessels, C. Reduction of Combusted Iron Using Hydrogen. Ph.D. Thesis, Eindhoven University of Technology, Eindhoven, The Netherlands, 2023.
117. Ali, A.; Zhang, N.; Santos, R.M. Mineral Characterization Using Scanning Electron Microscopy (SEM): A Review of the Fundamentals, Advancements, and Research Directions. *Appl. Sci.* **2023**, *13*, 12600. [[CrossRef](#)]

Disclaimer/Publisher's Note: The statements, opinions and data contained in all publications are solely those of the individual author(s) and contributor(s) and not of MDPI and/or the editor(s). MDPI and/or the editor(s) disclaim responsibility for any injury to people or property resulting from any ideas, methods, instructions or products referred to in the content.